

NASA TECHNICAL NOTE



NASA TN D-7739

NASA TN D-7739

CASE FILE
COPY

EVALUATION OF IMPORTANCE OF
LATERAL ACCELERATION DERIVATIVES
IN EXTRACTION OF LATERAL-DIRECTIONAL
DERIVATIVES AT HIGH ANGLES OF ATTACK

by Luat T. Nguyen

Langley Research Center

Hampton, Va. 23665



NATIONAL AERONAUTICS AND SPACE ADMINISTRATION • WASHINGTON, D. C. • OCTOBER 1974

1. Report No. NASA TN D-7739		2. Government Accession No.		3. Recipient's Catalog No.	
4. Title and Subtitle EVALUATION OF IMPORTANCE OF LATERAL ACCELERATION DERIVATIVES IN EXTRACTION OF LATERAL-DIRECTIONAL DERIVATIVES AT HIGH ANGLES OF ATTACK				5. Report Date October 1974	
				6. Performing Organization Code	
7. Author(s) Luat T. Nguyen				8. Performing Organization Report No. L-9689	
9. Performing Organization Name and Address NASA Langley Research Center Hampton, Va. 23665				10. Work Unit No. 501-26-04-02	
				11. Contract or Grant No.	
12. Sponsoring Agency Name and Address National Aeronautics and Space Administration Washington, D.C. 20546				13. Type of Report and Period Covered Technical Note	
				14. Sponsoring Agency Code	
15. Supplementary Notes					
16. Abstract <p>A theoretical investigation was conducted to determine the importance of the lateral acceleration ($\dot{\beta}$) derivatives in the extraction of lateral-directional stability derivatives for swept wing airplanes at high angles of attack. Representative values of lateral acceleration derivatives in yaw and roll ($C_{n\dot{\beta}}$ and $C_{l\dot{\beta}}$) were used in a computer program to generate representative flight motions at several angles of attack and altitudes. The computer-generated motions were then subjected to a parameter identification process based on a modified Newton-Raphson method. Two identification techniques were evaluated, one which included the $\dot{\beta}$ derivatives and one which neglected them.</p> <p>The results of the study indicate that omission of the $\dot{\beta}$ derivatives from mathematical models used in derivative-extraction techniques can produce erroneous values for the lateral-directional stability derivatives particularly at high angles of attack, where the $\dot{\beta}$ derivatives are large. The largest errors occur in the dynamic derivatives, but large errors may also occur in the static derivatives for cases in which the $\dot{\beta}$ derivatives have large effects on the flight motions of the airplane. In addition, the resulting identified mathematical models provide poor motion prediction as well as erroneous predictions of dynamic modal characteristics. These results strongly indicate that the effects of $\dot{\beta}$ derivatives should be considered in any attempt to extract lateral-directional aerodynamic parameters at high angles of attack.</p>					
17. Key Words (Suggested by Author(s)) Parameter estimation Derivative extraction High angle of attack			18. Distribution Statement Unclassified - Unlimited STAR Category 02		
19. Security Classif. (of this report) Unclassified		20. Security Classif. (of this page) Unclassified		21. No. of Pages 61	22. Price* \$3.75

EVALUATION OF IMPORTANCE OF LATERAL ACCELERATION
DERIVATIVES IN EXTRACTION OF LATERAL-DIRECTIONAL
DERIVATIVES AT HIGH ANGLES OF ATTACK

By Luat T. Nguyen
Langley Research Center

SUMMARY

A theoretical investigation was conducted to determine the importance of the lateral acceleration ($\dot{\beta}$) derivatives in the extraction of lateral-directional stability derivatives for swept wing airplanes at high angles of attack. Representative values of lateral acceleration derivatives in yaw and roll ($C_{n\dot{\beta}}$ and $C_{l\dot{\beta}}$) were used in a computer program to generate representative flight motions at several angles of attack and altitudes. The computer-generated motions were then subjected to a parameter identification process based on a modified Newton-Raphson method. Two identification techniques were evaluated, one which included the $\dot{\beta}$ derivatives and one which neglected them. The results of the identification procedures were compared with the actual values used to generate the flight motions.

The results of the study indicate that omission of the $\dot{\beta}$ derivatives from mathematical models used in derivative-extraction techniques can produce erroneous values for the lateral-directional stability derivatives particularly at high angles of attack, where the $\dot{\beta}$ derivatives are large. The largest errors occur in the dynamic derivatives, but large errors may also occur in the static derivatives for cases in which the $\dot{\beta}$ derivatives have large effects on the flight motions of the airplane. In addition, the resulting identified mathematical models provide poor motion prediction as well as erroneous predictions of dynamic stability characteristics. These results strongly indicate that the effects of $\dot{\beta}$ derivatives should be considered in any attempt to extract lateral-directional aerodynamic parameters at high angles of attack.

INTRODUCTION

The extraction of aerodynamic parameters from flight-test data has received increased attention over the past several years. Interest has been spurred primarily by the development of sophisticated parameter identification techniques which operate efficiently by using digital computers and which have been found to produce results superior

to those obtained from earlier estimation methods. A detailed discussion of the advantages of the new techniques is given in reference 1. These new techniques are generally classified as output-error methods and include the so-called modified Newton-Raphson and quasi-linearization methods. (See refs. 2 and 3.) Recently, a great deal of interest has been generated toward applying these parameter identification techniques to obtain estimates of aerodynamic derivatives for fighter airplanes in the high-angle-of-attack flight regime.

A primary consideration in this application is the mathematical model used in the identification process. It is well known that output-error methods can give very questionable results in the presence of process noise such as modeling errors. Up to the present time, the lateral-directional stability derivatives due to lateral acceleration ($\dot{\beta}$) have not been included in mathematical models used in the estimation of lateral-directional aerodynamic parameters. Such derivatives have usually been omitted because they are generally small at low angles of attack; moreover they are not easily estimated or measured in the wind tunnel. As indicated in reference 4, past wind-tunnel investigations employing testing equipment designed specifically to obtain the lateral acceleration derivatives have shown that large values for the derivatives $C_{l\dot{\beta}}$ and $C_{n\dot{\beta}}$ can be obtained for configurations with highly swept wings at high angles of attack. The past studies have also shown that these derivatives can have a major effect on the dynamic lateral-directional characteristics of a typical fighter at high angles of attack.

The present investigation was conducted to examine the importance of the lateral acceleration derivatives in the lateral-directional stability derivative identification process at high angles of attack. The effect of omitting these derivatives on the resulting parameter estimates was investigated by use of two linear dynamic models. One of the models included the effects of $C_{l\dot{\beta}}$ and $C_{n\dot{\beta}}$, whereas the second model represented the conventional approach in which these derivatives are neglected. The estimated aerodynamic parameters which resulted with and without the $C_{l\dot{\beta}}$ and $C_{n\dot{\beta}}$ terms were compared with the actual values of the respective parameters.

SYMBOLS

The lateral-directional derivatives presented herein are referred to the body axis system shown in figure 1. Dimensional quantities are presented in both U.S. Customary Units and the International System of Units. The subscript o indicates nominal value, and a dot over a symbol denotes a time derivative. The primed dimensional derivatives (for example, L'_p , N'_r , N'_β , etc.) are defined by equations (A9) to (A24) in the appendix.

b	wing span, m (ft)
C_L	lift coefficient, $\frac{\text{Aerodynamic lift force}}{\bar{q}S}$
C_l	rolling-moment coefficient about X body axis, $\frac{\text{Aerodynamic rolling moment}}{\bar{q}Sb}$
C_m	pitching-moment coefficient about Y body axis, $\frac{\text{Aerodynamic pitching moment}}{\bar{q}Sb}$
C_n	yawing-moment coefficient about Z body axis, $\frac{\text{Aerodynamic yawing moment}}{\bar{q}Sb}$
C_X	X-axis force coefficient along positive X body axis, $\frac{\text{Aerodynamic X-axis force}}{\bar{q}S}$
C_Y	Y-axis force coefficient along positive Y body axis, $\frac{\text{Aerodynamic Y-axis force}}{\bar{q}S}$
C_Z	Z-axis force coefficient along positive Z body axis, $\frac{\text{Aerodynamic Z-axis force}}{\bar{q}S}$
\bar{c}	wing mean aerodynamic chord, m (ft)
g	acceleration due to gravity, m/sec ² (ft/sec ²)
h	altitude, m (ft)
I_X	moment of inertia about X body axis, kg-m ² (slug-ft ²)
I_{XZ}	product of inertia with respect to X and Z body axes, kg-m ² (slug-ft ²)
I_Y	moment of inertia about Y body axis, kg-m ² (slug-ft ²)

I_Z	moment of inertia about Z body axis, $\text{kg}\cdot\text{m}^2$ (slug-ft ²)
m	airplane mass, kg (slugs)
P	period, sec
p	airplane roll rate about X body axis, rad/sec or deg/sec
q	airplane pitch rate about Y body axis, rad/sec or deg/sec
\bar{q}	free-stream dynamic pressure, N/m^2 (lb/ft ²)
r	yaw rate about Z body axis, rad/sec or deg/sec
S	wing area, m^2 (ft ²)
t	time, sec
$t_{1/2}$	time to damp to one-half, sec
u	component of airplane velocity along X body axis, m/sec (ft/sec)
V	airplane resultant velocity, m/sec (ft/sec)
v	component of airplane velocity along Y body axis, m/sec (ft/sec)
w	component of airplane velocity along Z body axis, m/sec (ft/sec)
X, Y, Z	airplane orthogonal body axes (see fig. 1)
α	angle of attack, rad or deg
β	angle of sideslip, rad or deg
δ_a	aileron deflection, positive for left roll, rad or deg
δ_e	elevator deflection, positive for nose-down control, rad or deg
δ_r	rudder deflection, positive for left yaw, rad or deg

θ, ϕ, ψ Euler angles, rad or deg

$$C_{l_p} = \frac{\partial C_l}{\partial \frac{pb}{2V}}$$

$$C_{l_r} = \frac{\partial C_l}{\partial \frac{rb}{2V}}$$

$$C_{l_{\dot{\beta}}} = \frac{\partial C_l}{\partial \frac{\dot{\beta}b}{2V}}$$

$$C_{l_{\beta}} = \frac{\partial C_l}{\partial \beta}$$

$$C_{l_{\delta_a}} = \frac{\partial C_l}{\partial \delta_a}$$

$$C_{l_{\delta_r}} = \frac{\partial C_l}{\partial \delta_r}$$

$$C_{m_q} = \frac{\partial C_m}{\partial \frac{q\bar{c}}{2V}}$$

$$C_{m_{\delta_e}} = \frac{\partial C_m}{\partial \delta_e}$$

$$C_{n_p} = \frac{\partial C_n}{\partial \frac{pb}{2V}}$$

$$C_{n_r} = \frac{\partial C_n}{\partial \frac{rb}{2V}}$$

$$C_{n_{\dot{\beta}}} = \frac{\partial C_n}{\partial \frac{\dot{\beta}b}{2V}}$$

$$C_{n_{\beta}} = \frac{\partial C_n}{\partial \beta}$$

$$C_{n_{\delta_a}} = \frac{\partial C_n}{\partial \delta_a}$$

$$C_{n_{\delta_r}} = \frac{\partial C_n}{\partial \delta_r}$$

$$C_{X_q} = \frac{\partial C_X}{\partial \frac{q\bar{c}}{2V}}$$

$$C_{X_{\delta_e}} = \frac{\partial C_X}{\partial \delta_e}$$

$$C_{Y_p} = \frac{\partial C_Y}{\partial \frac{pb}{2V}}$$

$$C_{Y_r} = \frac{\partial C_Y}{\partial \frac{rb}{2V}}$$

$$C_{Y_{\dot{\beta}}} = \frac{\partial C_Y}{\partial \frac{\dot{\beta}b}{2V}}$$

$$C_{Y_{\beta}} = \frac{\partial C_Y}{\partial \beta}$$

$$C_{Y_{\delta_a}} = \frac{\partial C_Y}{\partial \delta_a}$$

$$C_{Y_{\delta_r}} = \frac{\partial C_Y}{\partial \delta_r}$$

$$C_{Z_q} = \frac{\partial C_Z}{\partial \frac{q\bar{c}}{2V}}$$

$$C_{Z_{\delta_e}} = \frac{\partial C_Z}{\partial \delta_e}$$

$$L_p = \frac{\bar{q}Sb \left(\frac{b}{2V}\right) C_{l_p}}{I_X} \text{sec}^{-1}$$

$$L_r = \frac{\bar{q}Sb \left(\frac{b}{2V}\right) C_{l_r}}{I_X} \text{sec}^{-1}$$

$$L_{\dot{\beta}} = \frac{\bar{q}Sb \left(\frac{b}{2V}\right) C_{l_{\dot{\beta}}}}{I_X} \text{sec}^{-1}$$

$$L_{\beta} = \frac{\bar{q}Sb C_{l_{\beta}}}{I_X} \text{sec}^{-2}$$

$$L_{\delta_a} = \frac{\bar{q}Sb C_{l_{\delta_a}}}{I_X} \text{sec}^{-2}$$

$$L_{\delta_r} = \frac{\bar{q}Sb C_{l_{\delta_r}}}{I_X} \text{sec}^{-2}$$

$$N_p = \frac{\bar{q}Sb \left(\frac{b}{2V}\right) C_{n_p}}{I_Z} \text{sec}^{-1}$$

$$N_r = \frac{\bar{q}Sb \left(\frac{b}{2V}\right) C_{n_r}}{I_Z} \text{sec}^{-1}$$

$$N_{\dot{\beta}} = \frac{\bar{q}Sb \left(\frac{b}{2V}\right) C_{n_{\dot{\beta}}}}{I_Z} \text{sec}^{-1}$$

$$N_{\beta} = \frac{\bar{q}Sb C_{n_{\beta}}}{I_Z} \text{sec}^{-2}$$

$$N_{\delta_a} = \frac{\bar{q}Sb C_{n_{\delta_a}}}{I_Z} \text{sec}^{-2}$$

$$N_{\delta_r} = \frac{\bar{q}Sb C_{n_{\delta_r}}}{I_Z} \text{sec}^{-2}$$

$$Y_p = \frac{\bar{q}S \left(\frac{b}{2V}\right) C_{Y_p}}{mV}$$

$$Y_r = \frac{\bar{q}S \left(\frac{b}{2V}\right) C_{Y_r}}{mV}$$

$$Y_{\dot{\beta}} = \frac{\bar{q}S \left(\frac{b}{2V}\right) C_{Y_{\dot{\beta}}}}{mV}$$

$$Y_{\beta} = \frac{\bar{q}SC_{Y_{\beta}}}{mV} \text{sec}^{-1}$$

$$Y_{\delta_a} = \frac{\bar{q}SC_{Y_{\delta_a}}}{mV} \text{sec}^{-1}$$

$$Y_{\delta_r} = \frac{\bar{q}SC_{Y_{\delta_r}}}{mV} \text{sec}^{-1}$$

METHOD OF ANALYSIS

A schematic of the overall approach used in the investigation is shown in figure 2. Initially, mass and aerodynamic characteristics representative of a swept-wing fighter configuration were used as inputs to a nonlinear, six-degree-of-freedom computer program which generated time histories representative of flight data. The simulated flight data were then used in a Newton-Raphson parameter identification program which identified unknown lateral-directional stability derivatives by use of linear state-space models of the airplane. Two mathematical models were used for the parameter identification process. The first model properly represented $C_{n_{\dot{\beta}}}$ and $C_{l_{\dot{\beta}}}$, whereas the second model omitted these terms. The output of the Newton-Raphson program was a set of estimated aerodynamic derivatives extracted from the simulated flight data. Since the exact values for the aerodynamic derivatives were known inputs, the effects of mathematical model variations could be easily examined.

Simulation of Flight Data

The airplane configuration used in the investigation was the representative swept-wing fighter used in reference 4. The mass and dimensional characteristics of the configuration are listed in table I, and the aerodynamic data are presented in table II. The aerodynamic data were based on static and dynamic wind-tunnel tests of several configurations. It should be noted that the derivatives given in reference 4 were converted from the stability axis system to the body axis system for the present study. Furthermore, the study reported in reference 4 was restricted to lateral-directional considerations. In order to represent flight motions of an airplane with six degrees of freedom, representative values of longitudinal stability derivatives were chosen for the present study. The initial values of C_L were identical to those used in reference 4. Representative values of the control derivatives were also used in the investigation.

The variations of the lateral-directional stability derivatives with angle of attack are shown in figure 3. The derivatives $C_{n\dot{\beta}}$ and $C_{l\dot{\beta}}$ were relatively small at $\alpha = 10^\circ$, but the magnitudes of the derivatives increased rapidly as α was increased. At higher angles of attack, two variations of $C_{n\dot{\beta}}$ and $C_{l\dot{\beta}}$ were used to represent a range of static stability characteristics noted for fighter-type airplanes. The first variation (labeled case (a)) was representative of configurations which lose directional stability and effective dihedral at high angles of attack. This type of configuration usually exhibits a directional divergence ("nose slice") near stall. (See ref. 5.) The second variation (labeled case (b)) was representative of configurations which maintain stability at high angles of attack and usually have good stall characteristics.

The flight conditions for which data were generated are presented in table III. The initial conditions involved steady, level flight at angles of attack of 10° , 20° , and 30° at altitudes of sea level, 7620 m (25 000 ft), and 15 240 m (50 000 ft).

The dynamic lateral-directional stability characteristics of the airplane at these flight conditions are given in table IV. Part (a) of table IV presents values obtained when the terms $C_{n\dot{\beta}}$ and $C_{l\dot{\beta}}$ were included in the equations of motion to obtain the period and damping of the various modes. For comparison, stability characteristics obtained when both $C_{n\dot{\beta}}$ and $C_{l\dot{\beta}}$ were assumed to be zero are listed in part (b) of table IV. The differences between the calculated stability characteristics for the two sets of data are small at $\alpha = 10^\circ$ (where the values of $C_{n\dot{\beta}}$ and $C_{l\dot{\beta}}$ are small), fairly large at $\alpha = 20^\circ$ (where the derivatives are larger), and very large at $\alpha = 30^\circ$ (where the $\dot{\beta}$ derivatives were very large). These results show that the lateral acceleration derivatives can have a dominant effect on dynamic lateral-directional stability, particularly at high angles of attack, where these derivatives are large.

It will be noted that the results of table IV for $\alpha = 30^\circ$ (for example, runs 3(a) and 3(b)) show markedly different stability characteristics for the two sets of $C_{n\beta}$ and $C_{l\beta}$ used. For those designated (a), the unstable stability derivatives result in an aperiodic divergence ("nose slice"). The results obtained for those designated (b) indicate a stable airplane at $\alpha = 30^\circ$.

The aerodynamic and mass characteristics were used as inputs for a six-degree-of-freedom (6 DOF) nonlinear computer program which generated time histories of motions following control inputs. At each flight condition lateral-directional motion was initiated with the application of a rudder doublet followed by an aileron doublet. The airplane was then allowed a period of free motion during which the lateral-directional controls were neutralized. In generating these motions, an attempt was made to excite the lateral-directional modes sufficiently for proper derivative identification, whereas the motions were restricted so that the small perturbation assumption of the mathematical model was not invalidated. The motion program integrated the equations of motion at a fixed interval of 0.01 sec, and selected lateral-directional flight variables were provided as output on punched cards at 0.04 sec intervals for input to the identification program. Time histories of a typical flight are given in figure 4. The data show very little longitudinal motion; at the same time the lateral-directional modes were sufficiently excited without the motion becoming large enough to invalidate the linear, small perturbation model.

Estimation of Aerodynamic Parameters

The technique used for estimating the aerodynamic parameters from the computer-generated flight data was a modified Newton-Raphson method. A detailed description of the technique and computer program is found in reference 2. The technique computes a maximum-likelihood estimate of the unknown parameters of a linear, state-space model. Because measurement noise was not considered in this investigation, the maximum-likelihood estimate obtained is equivalent to one which minimizes the mean-square difference between the computed and measured response. The flight parameters that were input into the estimation program were the response variables p, r, β, ϕ and the control deflections δ_a and δ_r . These parameters are commonly measured during flight testing and are normally used for identification of aircraft lateral-directional aerodynamic parameters. No measurement of $\dot{\beta}$ was assumed to be available. Because the measurements were ideal (that is, no measurement noise was included in the generation of the flight data), differences between the measured and computed response variables p, r, β, ϕ were all weighted equally in the minimization process.

The linearized equations of motion used in the identification process are described in detail in the appendix. In the development of the mathematical model, the classical lateral-directional equations, including terms which were the result of the $\dot{\beta}$ derivatives, were put into state-space form to be compatible with the identification program. In this form, all the aerodynamic parameters appear as coefficients of the state variables p, r, β, ϕ and of the controls δ_a, δ_r . In matrix form, the equations are as follows:

$$\begin{bmatrix} \dot{p} \\ \dot{r} \\ \dot{\beta} \\ \dot{\phi} \end{bmatrix} = \begin{bmatrix} L'_p & L'_r & L'_\beta & L'_\phi \\ N'_p & N'_r & N'_\beta & N'_\phi \\ Y'_p & Y'_r & Y'_\beta & Y'_\phi \\ 1 & \tan \theta_0 & 0 & 0 \end{bmatrix} \begin{bmatrix} p \\ r \\ \beta \\ \phi \end{bmatrix} + \begin{bmatrix} L'_{\delta_a} & L'_{\delta_r} \\ N'_{\delta_a} & N'_{\delta_r} \\ Y'_{\delta_a} & Y'_{\delta_r} \\ 0 & 0 \end{bmatrix} \begin{bmatrix} \delta_a \\ \delta_r \end{bmatrix}$$

With this model, the $\dot{\beta}$ derivatives appear in all the primed derivatives but are explicitly identifiable as components of the coefficients of the bank angle ϕ . For example, the L'_ϕ and N'_ϕ terms are related to these derivatives as

$$L'_\phi = \frac{1}{1 - \frac{I_{XZ}^2}{I_X I_Z}} \left(\frac{g}{V_0} \cos \theta_0 \right) \left(L'_\beta + \frac{I_{XZ}}{I_X} N'_\beta \right)$$

and

$$N'_\phi = \frac{1}{1 - \frac{I_{XZ}^2}{I_X I_Z}} \left(\frac{g}{V_0} \cos \theta_0 \right) \left(\frac{I_{XZ}}{I_Z} L'_\beta + N'_\beta \right)$$

With the $\dot{\beta}$ derivatives identified, the other derivatives can be determined from the remaining primed derivatives by using the relationships given in the appendix.

Two models were used in the identification process. The first model included the values of $C_{l\dot{\beta}}$ and $C_{n\dot{\beta}}$, and estimates were obtained for the following parameters: $L'_p, L'_r, L'_\beta, L'_\phi, N'_p, N'_r, N'_\beta, N'_\phi, Y'_\beta, L'_{\delta_r}, L'_{\delta_a}, N'_{\delta_r},$ and N'_{δ_a} . The values of the derivatives $C_{Yp}, C_{Yr},$ and $C_{Y\delta_a}$ were assumed to be 0, and $C_{Y\delta_r}$ was known. Thus, $Y'_p, Y'_r, Y'_{\delta_a}, Y'_{\delta_r},$ and Y'_ϕ were also known and hence not included in the set of parameters to be identified. Once estimates of the dimensional primed derivatives

were obtained, the conventional nondimensional stability derivatives were derived by using the relationships given in the appendix and symbols section.

The second model used for parameter identification was one in which the values of $C_{l\dot{\beta}}$ and $C_{n\dot{\beta}}$ were assumed to be 0. The values of L'_ϕ and N'_ϕ were therefore assumed to be 0, and the computer-generated flight motions (with effects of the $\dot{\beta}$ derivatives present) were subjected to the conventional derivative identification process in which the $\dot{\beta}$ terms are neglected.

All the estimation runs were 10 sec in duration with a sample rate of 0.04 sec, for a total of 250 data points. In each case, the estimation program was allowed to operate until a convergence to a solution was established. Convergence always occurred within the first 10 iterations; however, to assure complete convergence, at least 15 iterations were made in every case. At the point at which the program was stopped, values of the gradient of the minimization function were typically on the order of 10^{-10} or less and indicated an accurate convergence.

RESULTS AND DISCUSSION

Effect of $\dot{\beta}$ Derivatives on Standard Deviation and Data Fit

Presented in table V are values of the primed dimensional lateral-directional derivatives and calculated estimates of the standard deviation for the two extraction techniques. The standard deviation is a measure of uncertainty in the extracted parameter, and a small value of the deviation in comparison with the magnitude of the parameter indicates a high degree of certainty in the estimate. The data of table V indicate that the standard deviations for the extracted derivatives were extremely small for all flight conditions for both identification techniques. Also, figures 5 to 8 show that the motions generated when either set of derivatives is used agree very closely with the actual "flight" motions from which the derivatives were extracted.

For the case of the unmodeled $\dot{\beta}$ derivatives, the foregoing results are completely misleading. A high degree of certainty is indicated by the standard deviation and time-history fits, even though omission of the $\dot{\beta}$ derivatives caused considerable errors in their estimated values. Moreover, when these derivatives were used to compute dynamic characteristics or to predict motions other than those used to extract the derivatives themselves, the results obtained were in error. (See discussion in the following section.)

Comparison of Extracted Derivatives With Actual Values

In figures 9 to 11, the values of the conventional nondimensional lateral-directional stability derivatives obtained by the two identification techniques are compared with the

actual values used in the computer-generated motions. The comparisons are shown at $\alpha = 10^\circ$, 20° , and 30° for altitudes of sea level, 7620 m (25 000 ft), and 15 240 m (50 000 ft). In general, the comparisons show that the errors caused by neglecting the $\dot{\beta}$ derivatives were small at $\alpha = 10^\circ$ (where the $\dot{\beta}$ derivatives were relatively small), larger at $\alpha = 20^\circ$, and very large at $\alpha = 30^\circ$ (where the $\dot{\beta}$ derivatives were large).

The largest errors were obtained in the dynamic derivatives, as might be expected. In addition, large errors in the static derivatives were also obtained for cases where the $\dot{\beta}$ derivatives were large. For example, for $\alpha = 30^\circ$ at sea level (fig. 9), omission of the $\dot{\beta}$ derivatives resulted in extracted values of $C_{l\beta}$ and $C_{n\beta}$ which were markedly different from the actual values. In fact, for case (a) (unstable values of $C_{n\beta}$ and $C_{l\beta}$ at $\alpha = 30^\circ$) the estimates were opposite in sign to the actual values. This particular result was caused possibly by the fact that the $\dot{\beta}$ derivatives provided substantial damping of the lateral-directional modes at $\alpha = 30^\circ$. (See table IV.)

When the flight motion created with the $\dot{\beta}$ derivatives was subjected to the identification process which omitted these terms, the technique forced the values of $C_{l\beta}$ and $C_{n\beta}$ to become stable in order to provide the increase in stability previously produced by the $\dot{\beta}$ derivatives. The values and trends estimated by the technique which neglected $C_{n\dot{\beta}}$ and $C_{l\dot{\beta}}$ were markedly different from those for the actual data used in generating the flight motions and indicated that severe errors are produced by omitting these terms in extraction processes at high angles of attack.

Also presented in figure 9 are values indicating the combined dynamic lateral-directional parameters normally measured during wind-tunnel forced-oscillation tests in roll and yaw. (See ref. 6.) The various combined derivatives (such as $C_{l_r} - C_{l\dot{\beta}} \cos \alpha$) are obtained rather than pure derivatives because of the physical constraints of wind-tunnel test procedures and equipment. It is interesting to note that the derivatives extracted by the identification technique which omitted the $\dot{\beta}$ derivatives agree reasonably well with these values. The reason for this agreement can be seen by examination of the equations relating the primed derivatives to the dimensional derivatives as shown in the appendix (eqs. (A13) to (A16)). For example, L_r' is given by

$$L_r' = \frac{1}{1 - \frac{I_{XZ}^2}{I_X I_Z}} \left[\left(L_r + \frac{I_{XZ}}{I_X} N_r \right) + L_{\dot{\beta}} (-\cos \alpha_o + Y_r) + \frac{I_{XZ}}{I_X} N_{\dot{\beta}} (-\cos \alpha_o + Y_r) \right]$$

Because I_{XZ}/I_X and Y_r are normally small, the dominant term in the right-hand side of the equation is $L_r - L_{\dot{\beta}} \cos \alpha_0$. Inspection of the remaining equations led to similar conclusions; that is,

$$L_p' \approx L_p + L_{\dot{\beta}} \sin \alpha_0$$

$$N_p' \approx N_p + N_{\dot{\beta}} \sin \alpha_0$$

$$N_r' \approx N_r - N_{\dot{\beta}} \cos \alpha_0$$

These results indicate that a derivative-extraction process which omits the $\dot{\beta}$ derivatives at high angles of attack (where they are large) produces values of the dynamic derivatives which tend to agree, at least in trend, with the combined derivatives obtained in wind-tunnel forced-oscillation tests. As stated earlier, however, such an extraction process not only provides erroneous estimates of the stability derivatives but also poor predictions of the airplane dynamic stability characteristics as defined by the period and time to damp to one-half amplitude of the characteristic modes. Shown in table VI are comparisons of lateral-directional stability characteristics computed by using the actual aerodynamic data and computed by using extracted data from the non- $\dot{\beta}$ -modeling technique. Note that the predicted modal characteristics differ considerably from the actual characteristics for the cases in which $\alpha = 30^\circ$, where the $\dot{\beta}$ derivatives are very large.

The fact that neither the modal characteristics nor the aerodynamic derivatives were correctly obtained when the $\dot{\beta}$ derivatives were omitted from the extraction procedure indicates that although the resulting identified mathematical models generate motions which closely match the flight motions from which they were extracted, these models could not be used to predict motions for other flight conditions or for different control inputs. For example, figure 12 presents comparative time histories of responses to an aileron doublet applied at the conditions of test run 3(a) ($\alpha = 30^\circ$, $h = 0$). A set of responses computed by using the results obtained from the non- $\dot{\beta}$ -modeling estimation technique is compared with the actual responses. As can be seen, the predicted responses do not agree well with the actual responses.

These results indicate that the omission of $\dot{\beta}$ derivatives from the derivative-extraction procedure at high angles of attack, where these derivatives are large, results in identified mathematical models which provide poor motion prediction as well as erroneous predictions of dynamic mode characteristics.

Also plotted in figures 9 to 11 are the results obtained when the $\dot{\beta}$ derivatives were included in the identification model in terms of L'_ϕ and N'_ϕ . As expected, the results agree closely with the actual values. It should be noted that the primary effects of the $\dot{\beta}$ derivatives appear in terms of L'_ϕ rather than N'_ϕ . This fact is reflected in the small values of N'_ϕ as shown in table V; note that in some cases N'_ϕ was fixed at 0 and not identified. On the other hand, values of L'_ϕ were large enough to be always easily identifiable. As shown in the figures, the values of $C_{n\dot{\beta}}$ and $C_{l\dot{\beta}}$ calculated from the L'_ϕ and N'_ϕ estimates were in excellent agreement with the actual values.

The data also reveal that the estimates of the control derivatives agree reasonably well with the actual values for both identification techniques. This result might be expected since the nonmodeling of $\dot{\beta}$ derivatives should not have a major effect on the identification of control parameters.

The data of figures 10 and 11 show that the extraction errors previously discussed for flight at sea level were present at higher altitudes, but the errors for $C_{n\dot{\beta}}$ and $C_{l\dot{\beta}}$ were less at the higher altitudes. The smaller error was probably caused by the fact that the $\dot{\beta}$ derivatives had a reduced effect on the stability of the airplane at higher altitudes. (See table IV.)

CONCLUSIONS

The results of a theoretical study to determine the importance of the lateral acceleration ($\dot{\beta}$) derivatives in the extraction of lateral-directional stability derivatives at high angles of attack has produced the following conclusions:

1. Omission of the $\dot{\beta}$ derivatives from mathematical models used to represent airplane flight conditions for derivative extraction at high angles of attack produces erroneous values for the lateral-directional stability derivatives at conditions where the $\dot{\beta}$ derivatives are large.
2. The largest errors occur in the dynamic derivatives, but large errors may also occur in the static derivatives in cases where the $\dot{\beta}$ derivatives have large effects on the flight motions of the airplane.
3. At high angles of attack, where the $\dot{\beta}$ effects are large, the mathematical models identified when the $\dot{\beta}$ derivatives are omitted provide poor motion prediction as well as erroneous predictions of dynamic mode characteristics.

4. The results strongly indicate that the effect of $\dot{\beta}$ derivatives should be considered in any attempt to extract lateral-directional aerodynamic parameters at high angles of attack.

Langley Research Center,
National Aeronautics and Space Administration,
Hampton, Va., July 17, 1974.

APPENDIX

LINEARIZED EQUATIONS OF MOTION USED IN IDENTIFICATION PROCESS

The general three-degree-of-freedom linearized lateral-directional equations of motion are (see ref. 7, for example):

$$\dot{\beta} + r \cos \alpha_0 - p \sin \alpha_0 - \frac{g}{V_0} \cos \theta_0 \phi = Y_\beta \beta + Y_{\dot{\beta}} \dot{\beta} + Y_p p + Y_r r + Y_{\delta_a} \delta_a + Y_{\delta_r} \delta_r \quad (\text{A1})$$

$$\dot{p} + \frac{I_Z - I_Y}{I_X} q_0 r - \frac{I_{XZ}}{I_X} (q_0 p + \dot{r}) = L_\beta \beta + L_{\dot{\beta}} \dot{\beta} + L_p p + L_r r + L_{\delta_a} \delta_a + L_{\delta_r} \delta_r \quad (\text{A2})$$

$$\dot{r} + \frac{I_Y - I_X}{I_Z} q_0 p + \frac{I_{XZ}}{I_Z} (q_0 r - \dot{p}) = N_\beta \beta + N_{\dot{\beta}} \dot{\beta} + N_p p + N_r r + N_{\delta_a} \delta_a + N_{\delta_r} \delta_r \quad (\text{A3})$$

$$\dot{\phi} = p + \tan \theta_0 r + q_0 \tan \theta_0 \phi \quad (\text{A4})$$

The $\dot{\beta}$, \dot{p} , and \dot{r} equations can also be expressed as

$$\dot{\beta} = \frac{Y_\beta}{1 - Y_{\dot{\beta}}} \beta + \frac{\sin \alpha_0 + Y_p}{1 - Y_{\dot{\beta}}} p + \frac{-\cos \alpha_0 + Y_r}{1 - Y_{\dot{\beta}}} r + \frac{\frac{g}{V_0} \cos \theta_0}{1 - Y_{\dot{\beta}}} \phi + \frac{Y_{\delta_a}}{1 - Y_{\dot{\beta}}} \delta_a + \frac{Y_{\delta_r}}{1 - Y_{\dot{\beta}}} \delta_r \quad (\text{A5})$$

$$\begin{aligned}
 \dot{p} = & \frac{1}{1 - \frac{I_{XZ}^2}{I_X I_Z}} \left[\left(L_{\dot{\beta}} + \frac{I_{XZ}}{I_X} N_{\dot{\beta}} \right) + \left(\frac{L_{\dot{\beta}} Y_{\dot{\beta}}}{1 - Y_{\dot{\beta}}} + \frac{I_{XZ}}{I_X} \frac{N_{\dot{\beta}} Y_{\dot{\beta}}}{1 - Y_{\dot{\beta}}} \right) \beta + \frac{1}{1 - \frac{I_{XZ}^2}{I_X I_Z}} \left[\left(L_p + \frac{I_{XZ}}{I_X} N_p \right) \right. \\
 & + \left. \left(\frac{I_{XZ}}{I_X} q_o - \frac{I_{XZ}}{I_X} \frac{I_Y - I_X}{I_Z} q_o \right) + \frac{L_{\dot{\beta}} (\sin \alpha_o + Y_p)}{1 - Y_{\dot{\beta}}} + \frac{I_{XZ}}{I_X} \frac{N_{\dot{\beta}} (\sin \alpha_o + Y_p)}{1 - Y_{\dot{\beta}}} \right] p \\
 & + \frac{1}{1 - \frac{I_{XZ}^2}{I_X I_Z}} \left[\left(L_r + \frac{I_{XZ}}{I_X} N_r \right) + \left(-\frac{I_Z - I_Y}{I_X} q_o - \frac{I_{XZ}^2}{I_X I_Z} q_o \right) + \frac{L_{\dot{\beta}} (-\cos \alpha_o + Y_r)}{1 - Y_{\dot{\beta}}} \right. \\
 & + \left. \frac{I_{XZ}}{I_X} \frac{N_{\dot{\beta}} (-\cos \alpha_o + Y_r)}{1 - Y_{\dot{\beta}}} \right] r + \frac{1}{1 - \frac{I_{XZ}^2}{I_X I_Z}} \left[\frac{g}{V_o} \cos \theta_o \left(\frac{L_{\dot{\beta}}}{1 - Y_{\dot{\beta}}} + \frac{I_{XZ}}{I_X} \frac{N_{\dot{\beta}}}{1 - Y_{\dot{\beta}}} \right) \right] \phi \\
 & + \frac{1}{1 - \frac{I_{XZ}^2}{I_X I_Z}} \left[\left(L_{\delta_a} + \frac{I_{XZ}}{I_X} N_{\delta_a} \right) + \left(\frac{L_{\dot{\beta}} Y_{\delta_a}}{1 - Y_{\dot{\beta}}} + \frac{I_{XZ}}{I_X} \frac{N_{\dot{\beta}} Y_{\delta_a}}{1 - Y_{\dot{\beta}}} \right) \right] \delta_a \\
 & + \frac{1}{1 - \frac{I_{XZ}^2}{I_X I_Z}} \left[\left(L_{\delta_r} + \frac{I_{XZ}}{I_X} N_{\delta_r} \right) + \left(\frac{L_{\dot{\beta}} Y_{\delta_r}}{1 - Y_{\dot{\beta}}} + \frac{I_{XZ}}{I_X} \frac{N_{\dot{\beta}} Y_{\delta_r}}{1 - Y_{\dot{\beta}}} \right) \right] \delta_r
 \end{aligned} \tag{A6}$$

$$\begin{aligned}
 \dot{r} = & \frac{1}{1 - \frac{I_{XZ}^2}{I_X I_Z}} \left[\left(\frac{I_{XZ}}{I_Z} L_{\beta} + N_{\beta} \right) + \left(\frac{I_{XZ}}{I_Z} \frac{L_{\dot{\beta}} Y_{\beta}}{1 - Y_{\dot{\beta}}} + \frac{N_{\dot{\beta}} Y_{\beta}}{1 - Y_{\dot{\beta}}} \right) \beta + \frac{1}{1 - \frac{I_{XZ}^2}{I_X I_Z}} \left[\left(\frac{I_{XZ}}{I_Z} L_p + N_p \right) \right. \right. \\
 & + \left. \left(-\frac{I_Y - I_X}{I_Z} q_o + \frac{I_{XZ}^2}{I_X I_Z} q_o \right) + \frac{I_{XZ}}{I_Z} \frac{L_{\dot{\beta}} (\sin \alpha_o + Y_p)}{1 - Y_{\dot{\beta}}} + \frac{N_{\dot{\beta}} (\sin \alpha_o + Y_p)}{1 - Y_{\dot{\beta}}} \right] p \\
 & + \frac{1}{1 - \frac{I_{XZ}^2}{I_X I_Z}} \left[\left(\frac{I_{XZ}}{I_Z} L_r + N_r \right) + \left(-\frac{I_{XZ}}{I_Z} q_o - \frac{I_{XZ}}{I_Z} \frac{I_Z - I_Y}{I_X} q_o \right) + \frac{I_{XZ}}{I_Z} \frac{L_{\dot{\beta}} (-\cos \alpha_o + Y_r)}{1 - Y_{\dot{\beta}}} \right. \\
 & + \left. \frac{N_{\dot{\beta}} (-\cos \alpha_o + Y_r)}{1 - Y_{\dot{\beta}}} \right] r + \frac{1}{1 - \frac{I_{XZ}^2}{I_X I_Z}} \left[\frac{g}{V_o} \cos \theta_o \left(\frac{I_{XZ}}{I_Z} \frac{L_{\dot{\beta}}}{1 - Y_{\dot{\beta}}} + \frac{N_{\dot{\beta}}}{1 - Y_{\dot{\beta}}} \right) \right] \phi \\
 & + \frac{1}{1 - \frac{I_{XZ}^2}{I_X I_Z}} \left[\left(\frac{I_{XZ}}{I_Z} L_{\delta_a} + N_{\delta_a} \right) + \left(\frac{I_{XZ}}{I_Z} \frac{L_{\dot{\beta}} Y_{\delta_a}}{1 - Y_{\dot{\beta}}} + \frac{N_{\dot{\beta}} Y_{\delta_a}}{1 - Y_{\dot{\beta}}} \right) \right] \delta_a \\
 & + \frac{1}{1 - \frac{I_{XZ}^2}{I_X I_Z}} \left[\left(\frac{I_{XZ}}{I_Z} L_{\delta_r} + N_{\delta_r} \right) + \left(\frac{I_{XZ}}{I_Z} \frac{L_{\dot{\beta}} Y_{\delta_r}}{1 - Y_{\dot{\beta}}} + \frac{N_{\dot{\beta}} Y_{\delta_r}}{1 - Y_{\dot{\beta}}} \right) \right] \delta_r
 \end{aligned} \tag{A7}$$

APPENDIX - Continued

By using matrix notation, equations (A4), (A5), (A6), and (A7) can be written as

$$\begin{bmatrix} \dot{p} \\ \dot{r} \\ \dot{\beta} \\ \dot{\phi} \end{bmatrix} = \begin{bmatrix} L'_p & L'_r & L'_\beta & L'_\phi \\ N'_p & N'_r & N'_\beta & N'_\phi \\ Y'_p & Y'_r & Y'_\beta & Y'_\phi \\ 1 & \tan \theta_0 & 0 & q_0 \tan \theta_0 \end{bmatrix} \begin{bmatrix} p \\ r \\ \beta \\ \phi \end{bmatrix} + \begin{bmatrix} L'_{\delta_a} & L'_{\delta_r} \\ N'_{\delta_a} & N'_{\delta_r} \\ Y'_{\delta_a} & Y'_{\delta_r} \\ 0 & 0 \end{bmatrix} \begin{bmatrix} \delta_a \\ \delta_r \end{bmatrix} \quad (\text{A8})$$

For this investigation $Y'_\beta = 0$, and the flight conditions were such that $q_0 = 0$. As a result, the primed derivatives can be written in terms of the dimensional derivatives as

$$L'_\phi = \frac{1}{1 - \frac{I_{XZ}^2}{I_X I_Z}} \left(\frac{g}{V_0} \cos \theta_0 \right) \left(L_\beta + \frac{I_{XZ}}{I_X} N_\beta \right) \quad (\text{A9})$$

$$N'_\phi = \frac{1}{1 - \frac{I_{XZ}^2}{I_X I_Z}} \left(\frac{g}{V_0} \cos \theta_0 \right) \left(\frac{I_{XZ}}{I_Z} L_\beta + N_\beta \right) \quad (\text{A10})$$

$$L'_\beta = \frac{1}{1 - \frac{I_{XZ}^2}{I_X I_Z}} \left[\left(L_\beta + \frac{I_{XZ}}{I_X} N_\beta \right) + \left(L_\beta Y_\beta + \frac{I_{XZ}}{I_X} N_\beta Y_\beta \right) \right] \quad (\text{A11})$$

$$N'_\beta = \frac{1}{1 - \frac{I_{XZ}^2}{I_X I_Z}} \left[\left(\frac{I_{XZ}}{I_Z} L_\beta + N_\beta \right) + \left(\frac{I_{XZ}}{I_Z} L_\beta Y_\beta + N_\beta Y_\beta \right) \right] \quad (\text{A12})$$

$$L'_p = \frac{1}{1 - \frac{I_{XZ}^2}{I_X I_Z}} \left[\left(L_p + \frac{I_{XZ}}{I_X} N_p \right) + L_\beta (\sin \alpha_0 + Y_p) + \frac{I_{XZ}}{I_X} N_\beta (\sin \alpha_0 + Y_p) \right] \quad (\text{A13})$$

APPENDIX - Continued

$$N'_p = \frac{1}{1 - \frac{I_{XZ}^2}{I_X I_Z}} \left[\left(\frac{I_{XZ}}{I_Z} L_p + N_p \right) + \frac{I_{XZ}}{I_Z} L_{\dot{\beta}} (\sin \alpha_o + Y_p) + N_{\dot{\beta}} (\sin \alpha_o + Y_p) \right] \quad (A14)$$

$$L'_r = \frac{1}{1 - \frac{I_{XZ}^2}{I_X I_Z}} \left[\left(L_r + \frac{I_{XZ}}{I_X} N_r \right) + L_{\dot{\beta}} (-\cos \alpha_o + Y_r) + \frac{I_{XZ}}{I_X} N_{\dot{\beta}} (-\cos \alpha_o + Y_r) \right] \quad (A15)$$

$$N'_r = \frac{1}{1 - \frac{I_{XZ}^2}{I_X I_Z}} \left[\left(\frac{I_{XZ}}{I_Z} L_r + N_r \right) + \frac{I_{XZ}}{I_Z} L_{\dot{\beta}} (-\cos \alpha_o + Y_r) + N_{\dot{\beta}} (-\cos \alpha_o + Y_r) \right] \quad (A16)$$

$$L'_{\delta_a} = \frac{1}{1 - \frac{I_{XZ}^2}{I_X I_Z}} \left[\left(L_{\delta_a} + \frac{I_{XZ}}{I_X} N_{\delta_a} \right) + \left(L_{\dot{\beta}} Y_{\delta_a} + \frac{I_{XZ}}{I_X} N_{\dot{\beta}} Y_{\delta_a} \right) \right] \quad (A17)$$

$$N'_{\delta_a} = \frac{1}{1 - \frac{I_{XZ}^2}{I_X I_Z}} \left[\left(\frac{I_{XZ}}{I_Z} L_{\delta_a} + N_{\delta_a} \right) + \left(\frac{I_{XZ}}{I_Z} L_{\dot{\beta}} Y_{\delta_a} + N_{\dot{\beta}} Y_{\delta_a} \right) \right] \quad (A18)$$

$$L'_{\delta_r} = \frac{1}{1 - \frac{I_{XZ}^2}{I_X I_Z}} \left[\left(L_{\delta_r} + \frac{I_{XZ}}{I_X} N_{\delta_r} \right) + \left(L_{\dot{\beta}} Y_{\delta_r} + \frac{I_{XZ}}{I_X} N_{\dot{\beta}} Y_{\delta_r} \right) \right] \quad (A19)$$

$$N'_{\delta_r} = \frac{1}{1 - \frac{I_{XZ}^2}{I_X I_Z}} \left[\left(\frac{I_{XZ}}{I_Z} L_{\delta_r} + N_{\delta_r} \right) + \left(\frac{I_{XZ}}{I_Z} L_{\dot{\beta}} Y_{\delta_r} + N_{\dot{\beta}} Y_{\delta_r} \right) \right] \quad (A20)$$

$$Y'_p = \sin \alpha_o + Y_p \quad (A21)$$

APPENDIX – Concluded

$$Y'_r = -\cos \alpha_0 + Y_r \quad (A22)$$

$$Y'_\beta = Y_\beta \quad (A23)$$

$$Y'_\phi = \frac{g}{V_0} \cos \theta_0 \quad (A24)$$

Note that the lateral acceleration derivatives appear in all the primed roll and yaw derivatives and that the parameters L'_ϕ and N'_ϕ are composed of them exclusively. Thus, identifying L'_ϕ and N'_ϕ makes possible the determination of C_{l_β} and C_{n_β} directly.

REFERENCES

1. Liff, Kenneth W.; and Taylor, Lawrence W., Jr.: Determination of Stability Derivatives From Flight Data Using a Newton-Raphson Minimization Technique. NASA TN D-6579, 1972.
2. Taylor, Lawrence W., Jr.; and Liff, Kenneth W.: Systems Identification Using a Modified Newton-Raphson Method - A FORTRAN Program. NASA TN D-6734, 1972.
3. Grove, Randall D.; Bowles, Roland L.; and Mayhew, Stanley C.: A Procedure for Estimating Stability and Control Parameters From Flight Test Data by Using Maximum Likelihood Methods Employing a Real-Time Digital System. NASA TN D-6735, 1972.
4. Campbell, John P.; and Woodling, Carroll H.: Calculated Effects of the Lateral Acceleration Derivatives on the Dynamic Lateral Stability of a Delta-Wing Airplane. NACA RM L54K26, 1955.
5. Anon.: Stall/Post-Stall/Spin Flight Test Demonstration Requirements for Airplanes. Mil. Specif. MIL-S-83691A (USAF), Mar. 31, 1971.
6. Grafton, Sue B.; and Libbey, Charles E.: Dynamic Stability Derivatives of a Twin-Jet Fighter Model for Angles of Attack From -10° to 110° . NASA TN D-6091, 1971.
7. Gainer, Thomas G.; and Hoffman, Sherwood: Summary of Transformation Equations and Equations of Motion Used in Free-Flight and Wind-Tunnel Data Reduction and Analysis. NASA SP-3070, 1972.

TABLE I.- MASS AND DIMENSIONAL CHARACTERISTICS OF AIRPLANE

Weight, N (lb)	101 641.4 (22 850)
Moments of inertia, kg-m ² (slug-ft ²)	
I _X	18 915.3 (13 951.39)
I _Y	94 906.0 (70 000.0)
I _Z	117 940.4 (86 989.51)
I _{XZ}	2071.0 (1527.50)
Wing dimensions:	
Span, m (ft)	11.61 (38.1)
Area, m ² (ft ²)	61.50 (662.0)
Mean aerodynamic chord, m (ft)	5.28 (17.32)

TABLE II.- AERODYNAMIC COEFFICIENTS

[Designations (a) and (b) on $C_{l\beta}$ and $C_{n\beta}$ indicate the two sets of data used for runs 3, 6, and 9]

Coefficient	Values of α of -				
	0°	10°	20°	30°	40°
Longitudinal					
C_X	-0.05	-0.03887	-0.13045	-0.31407	-0.46031
C_Z	0	-.41303	-.89882	-1.3360	-1.6917
C_m	.04	0	-.04	-.08	-.12
C_{Xq}	0	0	0	0	0
C_{Zq}	0	0	0	0	0
C_{mq}	-15.424	-17.967	-21.078	-15.155	-7.707
$C_{X\delta_e}$	0	0	0	0	0
$C_{Z\delta_e}$	0	0	0	0	0
$C_{m\delta_e}$	-.00977	-.01494	-.01505	-.01637	-.01384
Lateral directional					
$C_{l\beta}$ (a)	-0.0008433	-0.001159	-0.001474	0.00050	0.002474
$C_{l\beta}$ (b)	-.0008433	-.001159	-.001474	-.001366	-.001258
$C_{n\beta}$ (a)	.001095	.0008112	.0005278	-.000866	-.00226
$C_{n\beta}$ (b)	.001095	.0008112	.0005278	.000366	.0002042
$C_{Y\beta}$	-.009948	-.009948	-.009948	-.004992	-.000035
$C_{Y\dot{\beta}}$	0	0	0	0	0

TABLE II.- AERODYNAMIC COEFFICIENTS - Concluded

Coefficient	Values of α of -				
	0°	10°	20°	30°	40°
Lateral directional - Concluded					
$C_{l\dot{\beta}}$	0.18876	-0.15467	-0.49810	-1.1062	-1.7143
$C_{n\dot{\beta}}$	-.02614	.01334	.05282	.51603	.97924
C_{Yp}	0	0	0	0	0
C_{lp}	-.23229	-.17801	-.12373	.08990	.30353
C_{np}	.02147	.002115	-.01724	-.09036	-.16348
C_{Yr}	0	0	0	0	0
C_{lr}	.17648	.10212	.027761	.009641	-.00848
C_{nr}	-.13773	-.1720	-.20627	-.20990	-.21353
$C_{Y\delta_a}$	0	0	0	0	0
$C_{l\delta_a}$	-.00138	-.00102	-.00067	-.00045	-.0002
$C_{n\delta_a}$	0	0	0	0	0
$C_{Y\delta_r}$.00369	.00399	.00344	.00173	.00075
$C_{l\delta_r}$	0	0	0	0	0
$C_{n\delta_r}$	-.00184	-.00202	-.00167	-.00069	-.00021

TABLE III. - FLIGHT CONDITIONS

[Designations (a) and (b) on test runs 3, 6, and 9 correspond to the two data sets for $C_{l\beta}$ and $C_{n\beta}$ shown in table II]

Test run	α , deg	h, m (ft)	V, m/sec (ft/sec)
1	10	0 (0)	80.19 (263.09)
2	20	0 (0)	53.10 (174.21)
3 (a)	30	0 (0)	41.81 (137.18)
3 (b)	30	0 (0)	41.81 (137.18)
4	10	7 620 (25 000)	119.73 (392.80)
5	20	7 620 (25 000)	79.28 (260.10)
6 (a)	30	7 620 (25 000)	62.43 (204.81)
6 (b)	30	7 620 (25 000)	62.43 (204.81)
7	10	15 240 (50 000)	209.94 (672.37)
8	20	15 240 (50 000)	135.71 (445.23)
9 (a)	30	15 240 (50 000)	106.86 (350.58)
9 (b)	30	15 240 (50 000)	106.86 (350.58)

TABLE IV.- AIRPLANE DYNAMIC LATERAL-DIRECTIONAL STABILITY
CHARACTERISTICS AT STUDY FLIGHT CONDITIONS

[Designations (a) and (b) on test runs 3, 6, and 9 correspond to the two data sets for $C_{l\dot{\beta}}$ and $C_{n\dot{\beta}}$ shown in table II]

(a) $C_{n\dot{\beta}} \neq 0$; $C_{l\dot{\beta}} \neq 0$

Test run	Aperiodic modes		Oscillatory mode	
	$t_{1/2}$, sec	$t_{1/2}$, sec	P, sec	$t_{1/2}$, sec
1	14.91	0.429	4.538	1.409
2	5.393	.915	5.403	.8907
3 (a)	-3.821	.254	53.93	2.369
3 (b)	6.754	1.503	9.634	.5401
4	21.91	.72	4.21	1.79
5	7.97	1.44	4.74	1.30
6 (a)	-2.58	.34	49.13	4.52
6 (b)	9.83	1.98	6.06	.83
7	37.17	1.317	3.995	2.821
8	13.56	2.515	4.476	2.204
9 (a)	-1.55	.451	78.30	10.36
9 (b)	16.62	3.243	5.218	1.430

(b) $C_{n\dot{\beta}} = 0$; $C_{l\dot{\beta}} = 0$

Test run	Aperiodic modes		Oscillatory mode	
	$t_{1/2}$, sec	$t_{1/2}$, sec	P, sec	$t_{1/2}$, sec
1	14.73	0.451	4.345	1.777
2	5.282	.956	4.479	3.714
3 (a)	-.569	.979	30.65	5.69
3 (b)	6.50	1.49	4.69	-1.66
4	21.78	.73	4.12	2.29
5	7.89	1.46	4.41	5.34
6 (a)	-.63	.92	46.36	7.75
6 (b)	9.67	2.05	4.78	-2.36
7	37.1	1.33	3.97	3.61
8	13.5	2.52	4.38	8.96
9 (a)	.857	-.678	80.4	12.7
9 (b)	16.5	3.31	4.85	-3.91

TABLE V.- ESTIMATES OF AERODYNAMIC PARAMETERS OBTAINED
FOR STUDY FLIGHT CONDITIONS

(a) $\alpha = 10^0$; $h = 0$

Parameter	Unmodeled $\dot{\beta}$ effects		Modeled $\dot{\beta}$ effects	
	Estimated value	Deviation	Estimated value	Deviation
L'_p	-2.3673	0.0009	-2.2726	0.0007
L'_r	2.7979	.0004	2.8093	.0004
L'_β	-10.0707	.0001	-9.5129	.0001
L'_ϕ	-----	-----	-.1792	.0006
L'_{δ_a}	-9.8037	.0003	-9.6780	.0003
L'_{δ_r}	-.3675	.0007	-.3447	.0007
N'_p	-.0752	.0018	-.0285	.0016
N'_r	-.3270	.0018	-.2634	.0010
N'_β	.6789	.0004	.9530	.0003
N'_ϕ	-----	-----	.0018	.0046
N'_{δ_a}	-.2459	.0007	-.1547	.0005
N'_{δ_r}	-2.7796	.0012	-2.7645	.0011
Y'_β	-.2108	.0015	-.1689	.0009

TABLE V.- ESTIMATES OF AERODYNAMIC PARAMETERS OBTAINED
FOR STUDY FLIGHT CONDITIONS - Continued

(b) $\alpha = 20^{\circ}$; $h = 0$

Parameter	Unmodeled $\dot{\beta}$ effects		Modeled $\dot{\beta}$ effects	
	Estimated value	Deviation	Estimated value	Deviation
L'_p	-2.2062	0.0008	-2.1162	0.0008
L'_r	3.1723	.0003	3.5756	.0003
L'_β	-6.4493	.0002	-5.0728	.0001
L'_ϕ	-----	-----	-.6306	.0007
L'_{δ_a}	-2.5916	.0010	-2.5133	.0010
L'_{δ_r}	-.2994	.0012	-.2245	.0013
N'_p	-.0748	.0018	-.0359	.0018
N'_r	-.3617	.0009	-.2286	.0007
N'_β	.0569	.0007	.2157	.0008
N'_ϕ	-----	-----	.0019	.0045
N'_{δ_a}	-.0273	.0021	-.0441	.0020
N'_{δ_r}	-.9885	.0019	-1.0002	.0017
Y'_β	-.3062	.0009	-.1076	.0007

TABLE V.- ESTIMATES OF AERODYNAMIC PARAMETERS OBTAINED
FOR STUDY FLIGHT CONDITIONS - Continued

(c) $\alpha = 30^{\circ}$; case (a), $h = 0$

Parameter	Unmodeled $\dot{\beta}$ effects		Modeled $\dot{\beta}$ effects	
	Estimated value	Deviation	Estimated value	Deviation
L'_p	-2.5012	0.0004	-2.6800	0.0004
L'_r	4.2980	.0002	5.5711	.0001
L'_β	-2.7270	.0001	1.4812	.0001
L'_ϕ	-----	-----	-1.3440	.0003
L'_{δ_a}	-.9977	.0015	-1.0883	.0013
L'_{δ_r}	-.2539	.0023	-.1059	.0017
N'_p	.0671	.0012	.0948	.0012
N'_r	-.5092	.0005	-.4753	.0004
N'_β	.1166	.0006	-.2930	.0004
N'_ϕ	-----	-----	.0680	.0012
N'_{δ_a}	-.0561	.0028	-.0222	.0027
N'_{δ_r}	-.2560	.0045	-.2514	.0038
Y'_β	-.0707	.0006	-.0301	.0007

TABLE V.- ESTIMATES OF AERODYNAMIC PARAMETERS OBTAINED
FOR STUDY FLIGHT CONDITIONS – Continued

(d) $\alpha = 30^{\circ}$; case (b); $h = 0$

Parameter	Unmodeled $\dot{\beta}$ effects		Modeled $\dot{\beta}$ effects	
	Estimated value	Deviation	Estimated value	Deviation
L'_p	-2.3405	0.0004	-2.6388	0.0004
L'_r	4.1234	.0002	5.5176	.0001
L'_β	-5.6868	.0002	-2.9549	.0001
L'_ϕ	-----	-----	-1.2843	.0005
L'_{δ_a}	-1.0005	.0015	-1.0628	.0013
L'_{δ_r}	-.1750	.0031	-.1146	.0027
N'_p	-.0585	.0014	.1086	.0009
N'_r	-.3651	.0006	-.5053	.0004
N'_β	.2263	.0005	.0678	.0007
N'_ϕ	-----	-----	.0751	.0018
N'_{δ_a}	-.0790	.0026	-.0175	.0022
N'_{δ_r}	-.2346	.0050	-.2518	.0045
Y'_β	-.3888	.0005	-.0431	.0004

TABLE V.- ESTIMATES OF AERODYNAMIC PARAMETERS OBTAINED
FOR STUDY FLIGHT CONDITIONS - Continued

(e) $\alpha = 10^0$; $h = 7620$ m (25 000 ft)

Parameter	Unmodeled $\dot{\beta}$ effects		Modeled $\dot{\beta}$ effects	
	Estimated value	Deviation	Estimated value	Deviation
L'_p	-1.4971	0.0011	-1.4993	0.0011
L'_r	1.9585	.0003	1.8433	.0003
L'_β	-9.6108	.0001	-9.6758	.0001
L'_ϕ	-----	-----	-.0902	.0008
L'_{δ_a}	-9.4561	.0004	-9.3159	.0003
L'_{δ_r}	-.3108	.0004	-.3098	.0004
N'_p	-.0168	.0030	-.0219	.0029
N'_r	-.1801	.0007	-.1788	.0007
N'_β	.9676	.0004	.9364	.0004
N'_ϕ	-----	-----	0 (fixed)	-----
N'_{δ_a}	-.1416	.0009	-.1548	.0009
N'_{δ_r}	-2.7576	.0007	-2.7569	.0007
Y'_β	-.1108	.0009	-.1133	.0009

TABLE V.- ESTIMATES OF AERODYNAMIC PARAMETERS OBTAINED
FOR STUDY FLIGHT CONDITIONS – Continued

(f) $\alpha = 20^\circ$; h = 7620 m (25 000 ft)

Parameter	Unmodeled $\dot{\beta}$ effects		Modeled $\dot{\beta}$ effects	
	Estimated value	Deviation	Estimated value	Deviation
L'_p	-1.4468	0.0014	-1.4148	0.0013
L'_r	2.2520	.0003	2.3769	.0003
L'_β	-5.8514	.0003	-5.3193	.0002
L'_ϕ	-----	-----	-.2804	.0006
L'_{δ_a}	-2.5535	.0014	-2.5149	.0014
L'_{δ_r}	-.2092	.0010	-.1569	.0010
N'_p	-.0373	.0027	.0001	.0180
N'_r	-.1979	.0009	-.0238	.0026
N'_β	.2029	.0010	-.1542	.0008
N'_ϕ	-----	-----	.2184	.0010
N'_{δ_a}	-.0306	.0026	-.0441	.0025
N'_{δ_r}	-.9822	.0015	-1.0015	.0013
Y'_β	-.1080	.0013	-.0731	.0009

TABLE V.- ESTIMATES OF AERODYNAMIC PARAMETERS OBTAINED
FOR STUDY FLIGHT CONDITIONS - Continued

(g) $\alpha = 30^{\circ}$; case (a); h = 7620 m (25 000 ft)

Parameter	Unmodeled $\dot{\beta}$ effects		Modeled $\dot{\beta}$ effects	
	Estimated value	Deviation	Estimated value	Deviation
L'_p	-1.8445	0.0005	-1.7521	0.0005
L'_r	3.0631	.0003	3.6494	.0002
L'_β	1.5987	.0003	1.2553	.0003
L'_ϕ	-----	-----	-.5728	.0011
L'_{δ_a}	-1.4961	.0010	-1.0478	.0010
L'_{δ_r}	-.1425	.0030	-.0653	.0027
N'_p	.2314	.0011	.0713	.0014
N'_r	-.7828	.0006	-.3350	.0005
N'_β	-.6284	.0007	-.3079	.0011
N'_ϕ	-----	-----	.0347	.0025
N'_{δ_a}	.1185	.0017	-.0197	.0022
N'_{δ_r}	-.3047	.0056	-.2544	.0048
Y'_β	.0459	.0015	-.0303	.0016

TABLE V.- ESTIMATES OF AERODYNAMIC PARAMETERS OBTAINED
FOR STUDY FLIGHT CONDITIONS - Continued

(h) $\alpha = 30^{\circ}$; case (b); $h = 7620$ m (25 000 ft)

Parameter	Unmodeled $\dot{\beta}$ effects		Modeled $\dot{\beta}$ effects	
	Estimated value	Deviation	Estimated value	Deviation
L'_p	-1.6048	0.0006	-1.7566	0.0006
L'_r	3.1503	.0003	3.6604	.0002
L'_β	-3.8954	.0003	-3.0854	.0002
L'_ϕ	-----	-----	-.5719	.0009
L'_{δ_a}	-1.0242	.0018	-1.0545	.0017
L'_{δ_r}	-.1043	.0040	-.0653	.0038
N'_p	-.0540	.0022	.0723	.0013
N'_r	-.2150	.0009	-.3355	.0006
N'_β	.1365	.0008	.0754	.0008
N'_ϕ	-----	-----	.0337	.0042
N'_{δ_a}	-.0488	.0028	-.0177	.0023
N'_{δ_r}	-.2327	.0060	-.2544	.0051
Y'_β	-.3266	.0006	-.0278	.0005

TABLE V.- ESTIMATES OF AERODYNAMIC PARAMETERS OBTAINED
FOR STUDY FLIGHT CONDITIONS - Continued

(i) $\alpha = 10^0$; h = 15 240 m (50 000 ft)

Parameter	Unmodeled $\dot{\beta}$ effects		Modeled $\dot{\beta}$ effects	
	Estimated value	Deviation	Estimated value	Deviation
L'_p	-0.8720	0.0018	-0.8708	0.0018
L'_r	1.0157	.0004	1.1068	.0004
L'_β	-9.9465	.0002	-9.6943	.0002
L'_ϕ	-----	-----	-.0313	.0025
L'_{δ_a}	-9.5132	.0004	-9.5374	.0004
L'_{δ_r}	-.3477	.0005	-.2782	.0005
N'_p	-.0107	.0083	-.0134	.0080
N'_r	-.1351	.0016	-.0981	.0012
N'_β	.9089	.0009	.9330	.0008
N'_ϕ	-----	-----	0 (fixed)	-----
N'_{δ_a}	-.1213	.0013	-.1318	.0013
N'_{δ_r}	-2.7660	.0009	-2.7455	.0009
Y'_β	-.0695	.0011	-.0717	.0011

TABLE V.- ESTIMATES OF AERODYNAMIC PARAMETERS OBTAINED
FOR STUDY FLIGHT CONDITIONS - Continued

(j) $\alpha = 20^{\circ}$; h = 15 240 m (50 000 ft)

Parameter	Unmodeled $\dot{\beta}$ effects		Modeled $\dot{\beta}$ effects	
	Estimated value	Deviation	Estimated value	Deviation
L'_p	-0.8218	0.0022	-0.8219	0.0022
L'_r	1.2189	.0006	1.4085	.0005
L'_β	-5.7610	.0004	-5.3652	.0003
L'_ϕ	-----	-----	-.0992	.0018
L'_{δ_a}	-2.4817	.0015	-2.4947	.0015
L'_{δ_r}	-.1540	.0017	-.1210	.0017
N'_p	-.0237	.0045	-.0163	.0048
N'_r	-.1132	.0021	-.0766	.0021
N'_β	.1538	.0012	.2206	.0010
N'_ϕ	-----	-----	0 (fixed)	-----
N'_{δ_a}	-.0279	.0038	-.0423	.0036
N'_{δ_r}	-.9843	.0025	-.9938	.0026
Y'_β	-.1036	.0013	-.0518	.0013

TABLE V.- ESTIMATES OF AERODYNAMIC PARAMETERS OBTAINED
FOR STUDY FLIGHT CONDITIONS - Continued

(k) $\alpha = 30^{\circ}$; case (a); h = 15 240 m (50 000 ft)

Parameter	Unmodeled $\dot{\beta}$ effects		Modeled $\dot{\beta}$ effects	
	Estimated value	Deviation	Estimated value	Deviation
L'_p	-0.9612	0.0012	-1.0491	0.0012
L'_r	1.8218	.0006	2.1342	.0005
L'_β	.6438	.0003	1.1889	.0004
L'_ϕ	-----	-----	-.2059	.0014
L'_{δ_a}	-1.1254	.0014	-1.0803	.0015
L'_{δ_r}	-.0968	.0043	-.0367	.0034
N'_p	.0848	.0019	.0397	.0020
N'_r	-.3068	.0011	-.1925	.0008
N'_β	-.3870	.0005	-.3009	.0006
N'_ϕ	-----	-----	.0130	.0024
N'_{δ_a}	.0254	.0018	-.0205	.0022
N'_{δ_r}	-.2661	.0061	-.2555	.0048
Y'_β	-.0371	.0008	-.0167	.0012

TABLE V.- ESTIMATES OF AERODYNAMIC PARAMETERS OBTAINED
FOR STUDY FLIGHT CONDITIONS – Concluded

(1) $\alpha = 30^{\circ}$; case (b); h = 15 240 m (50 000 ft)

Parameter	Unmodeled $\dot{\beta}$ effects		Modeled $\dot{\beta}$ effects	
	Estimated value	Deviation	Estimated value	Deviation
L'_p	-0.9764	0.0011	-1.0214	0.0011
L'_r	1.9202	.0005	2.1204	.0004
L'_β	-3.4293	.0005	-3.1528	.0004
L'_ϕ	-----	-----	-.1942	.0022
L'_{δ_a}	-1.0326	.0016	-1.0431	.0015
L'_{δ_r}	-.0615	.0052	-.0401	.0049
N'_p	-.0370	.0028	.0427	.0020
N'_r	-.0747	.0014	-.1964	.0009
N'_β	.1194	.0009	.0787	.0009
N'_ϕ	-----	-----	.0119	.0099
N'_{δ_a}	-.0556	.0021	-.0173	.0018
N'_{δ_r}	-.2360	.0089	-.2555	.0063
Y'_β	-.1487	.0009	-.0156	.0008

TABLE VI.- COMPARISON OF ACTUAL STABILITY CHARACTERISTICS
 WITH THOSE COMPUTED FROM ESTIMATION RESULTS
 FOR NON- $\dot{\beta}$ -MODELING CASE

Test run	Actual characteristics				Non- $\dot{\beta}$ -modeling characteristics			
	Aperiodic mode		Oscillatory mode		Aperiodic mode		Oscillatory mode	
	$t_{1/2}$, sec	$t_{1/2}$, sec	P, sec	$t_{1/2}$, sec	$t_{1/2}$, sec	$t_{1/2}$, sec	P, sec	$t_{1/2}$, sec
1	14.9	0.429	4.54	1.41	23.3	0.365	4.69	1.42
2	5.39	.915	5.40	.891	4.47	.588	5.62	.90
3 (a)	-3.82	.254	53.9	2.37	2.66	.342	15.7	1.75
3 (b)	6.75	1.50	9.63	.540	13.9	.855	4.45	.619

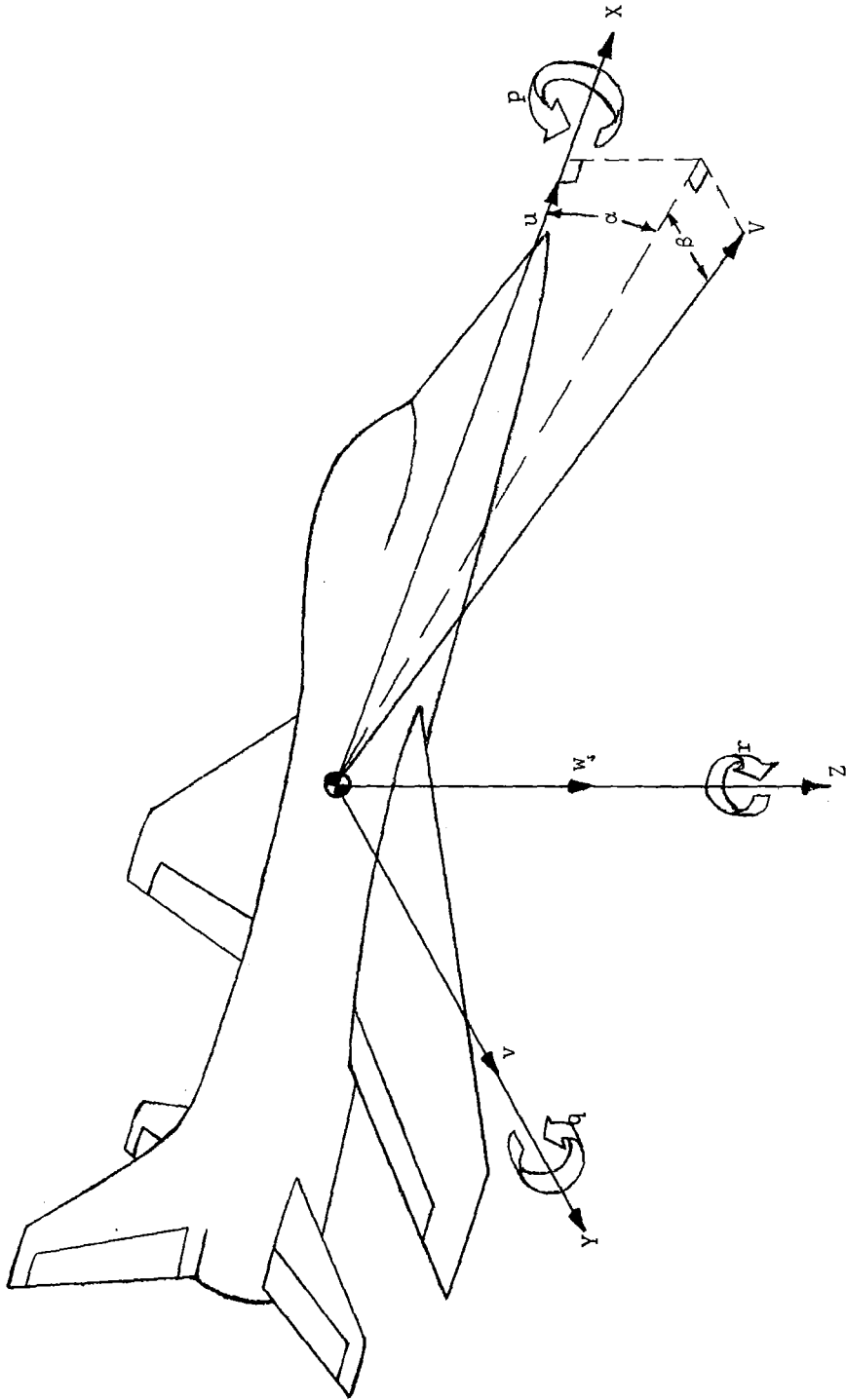


Figure 1.- The body system of axes.

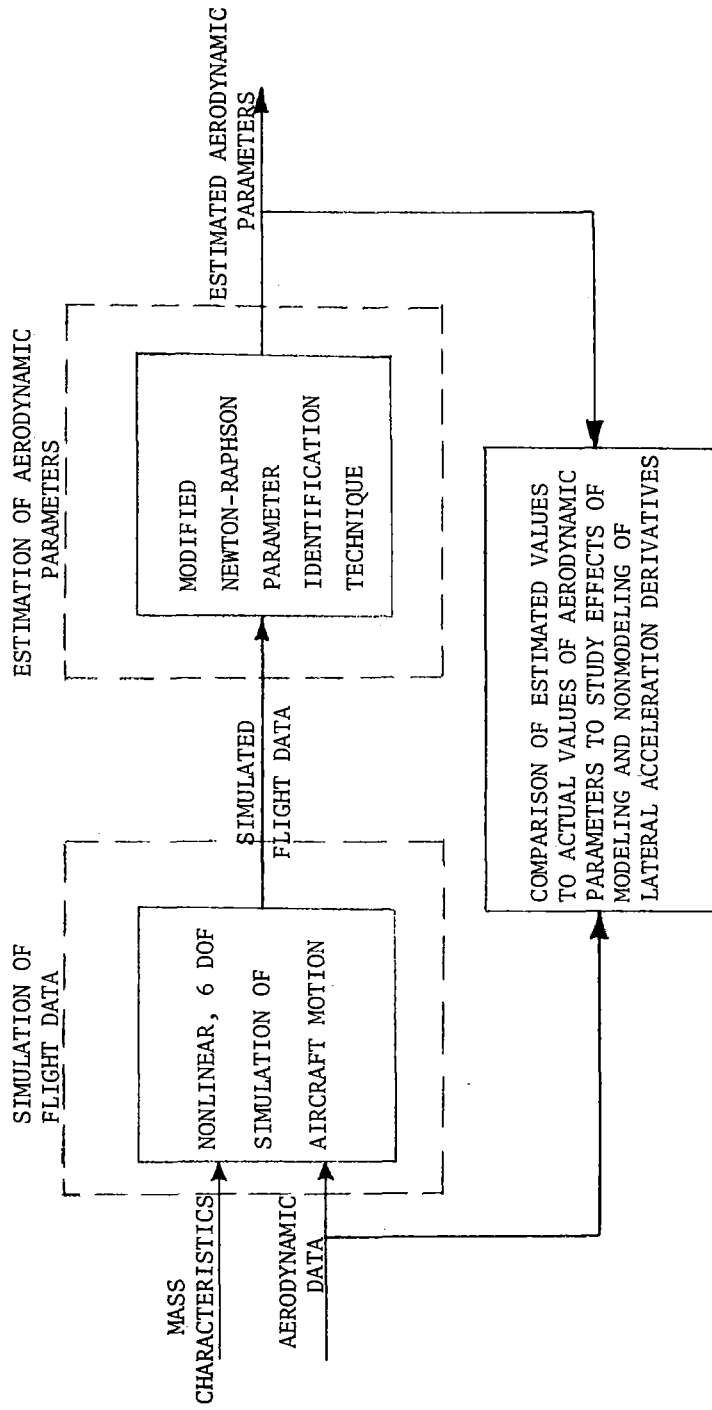


Figure 2.- Schematic of overall method of analysis.

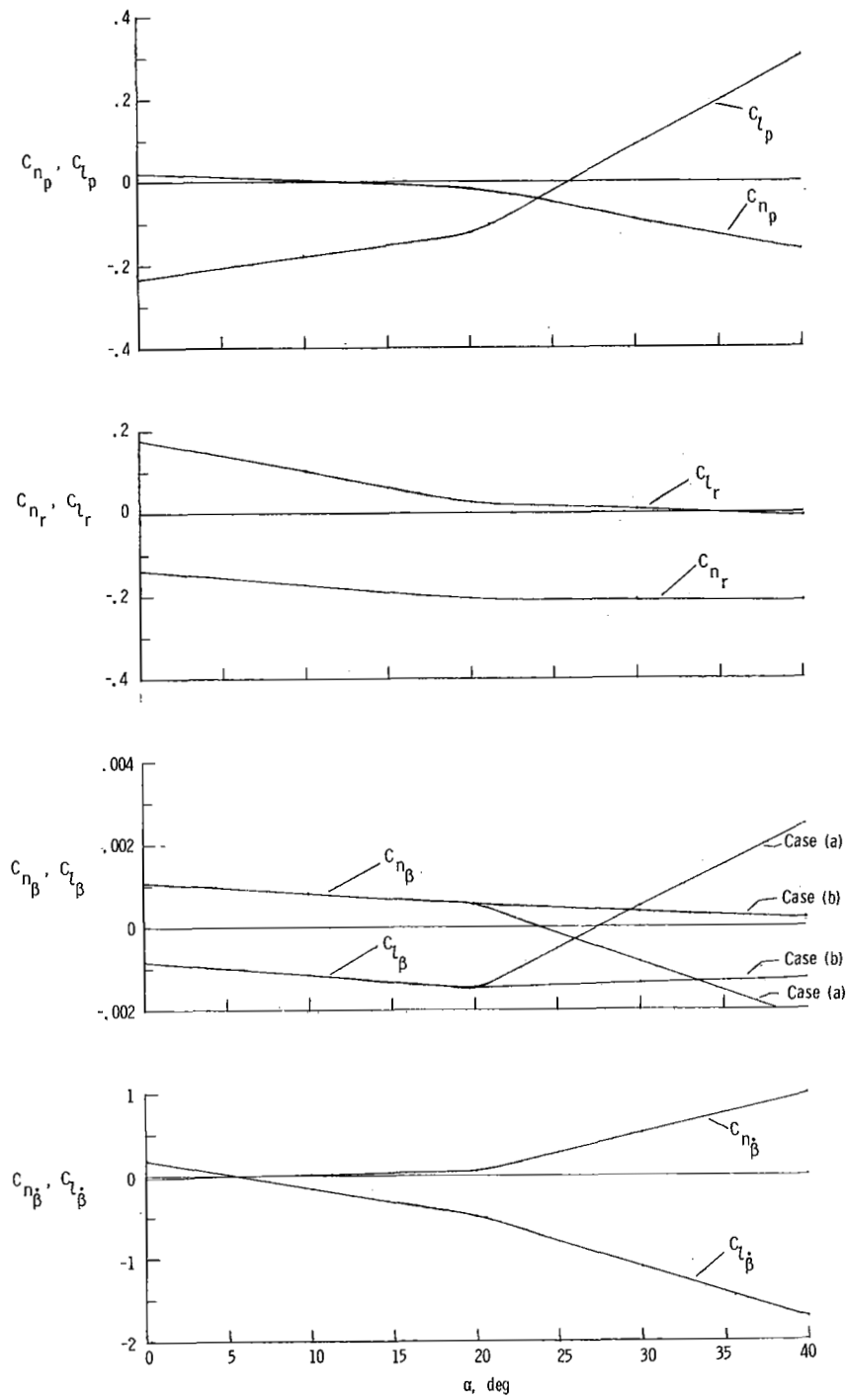


Figure 3.- Variation of lateral-directional stability derivatives with angle of attack.

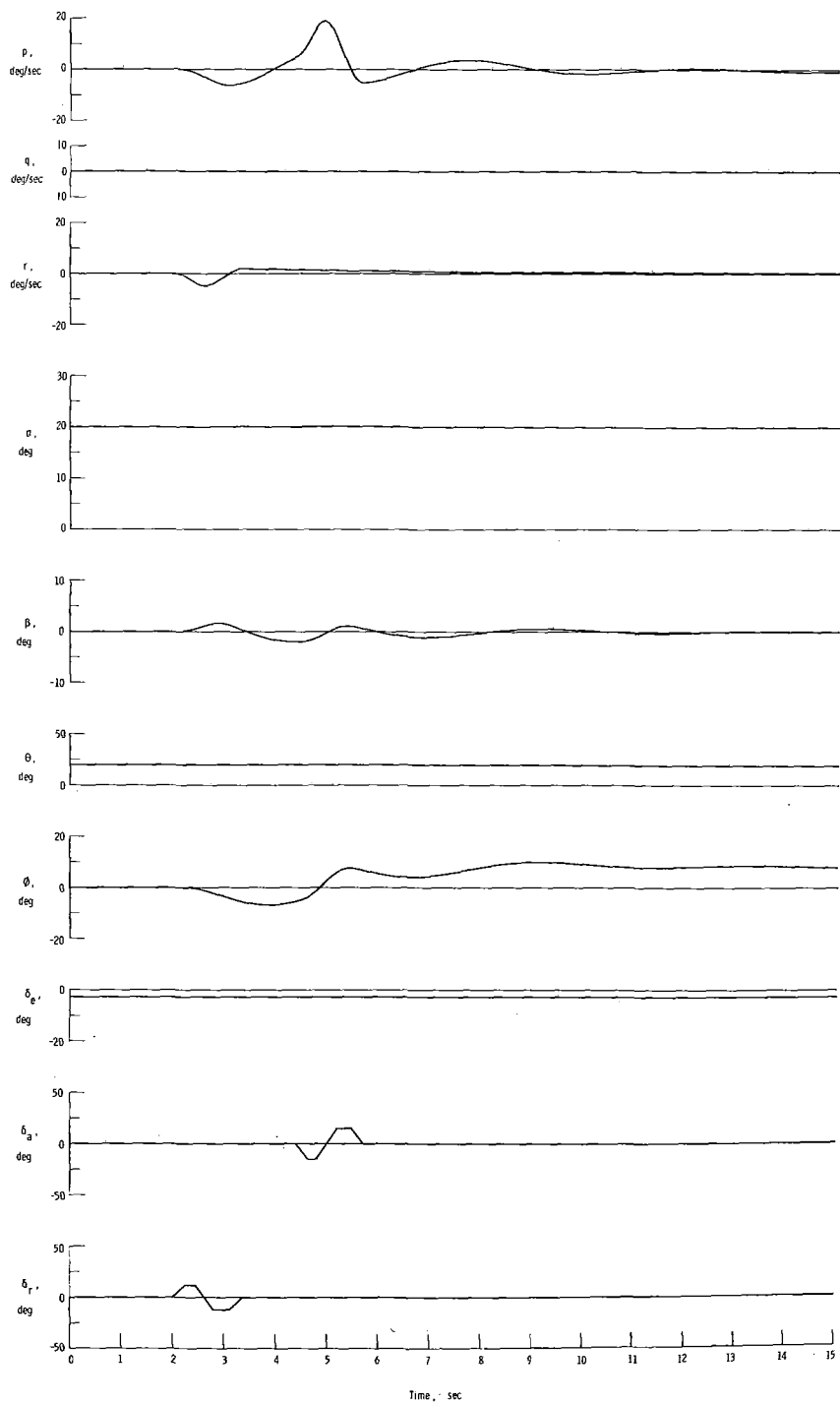
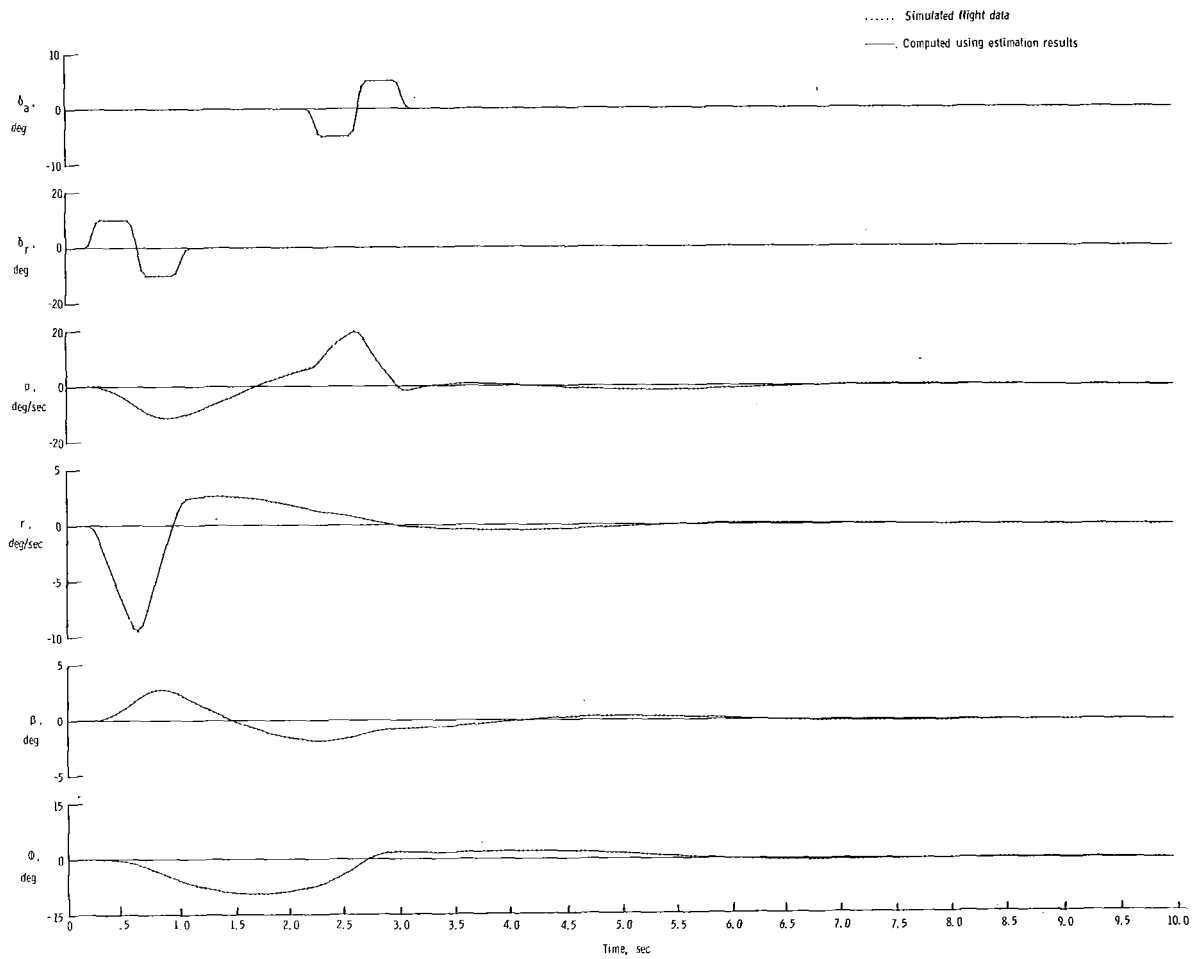
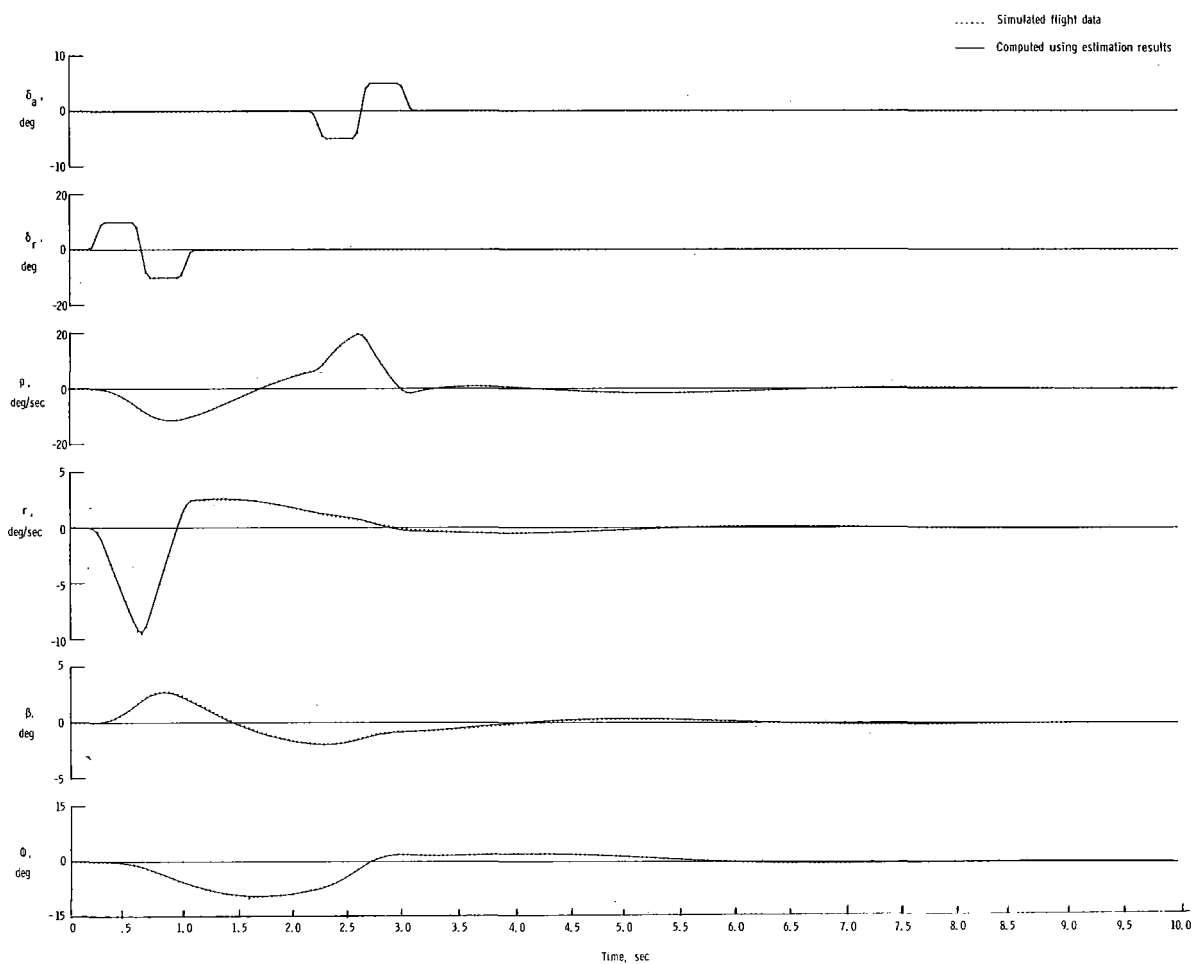


Figure 4.- Time histories of a typical simulated flight motion.



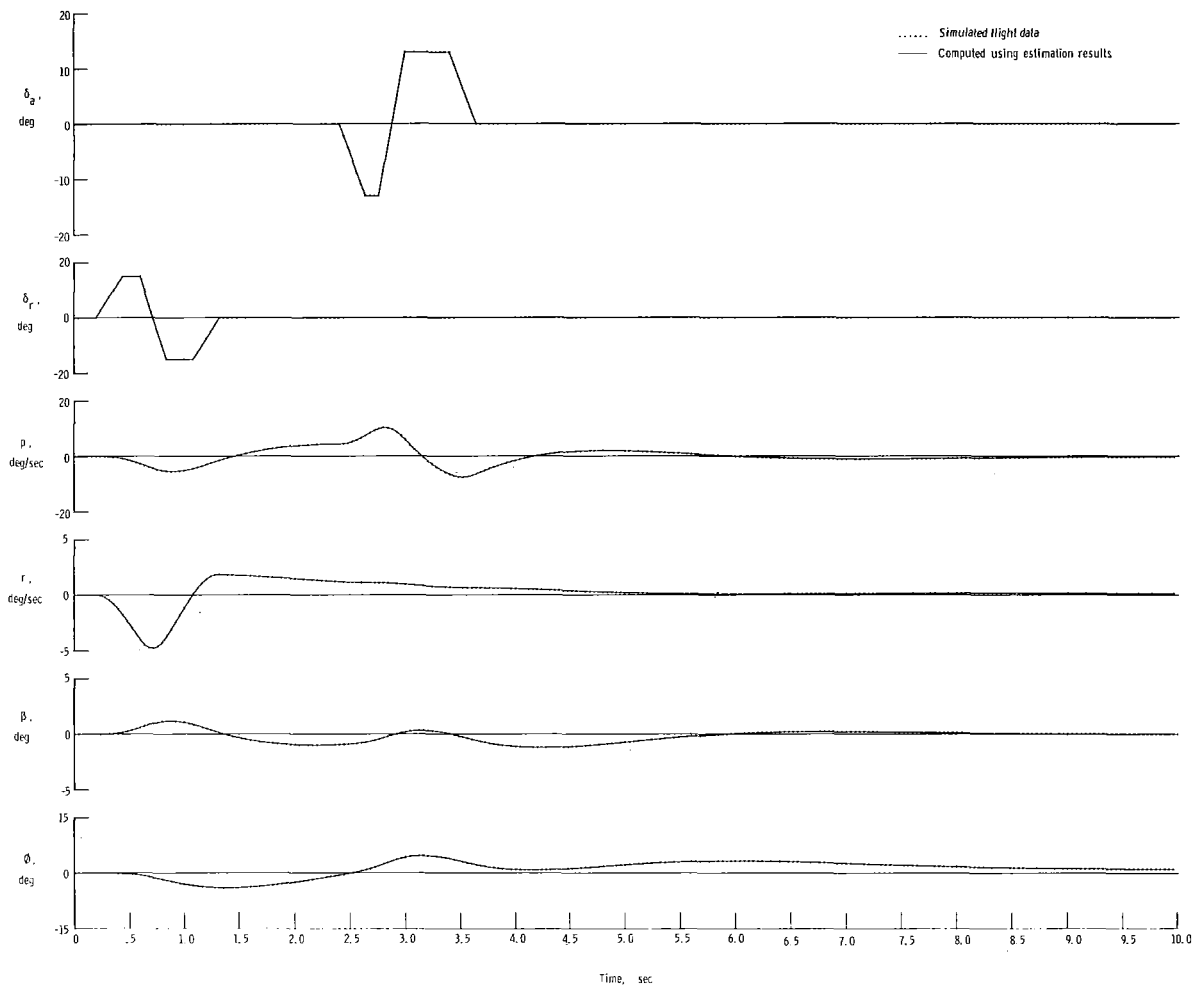
(a) Modeled $\hat{\beta}$ effects.

Figure 5.- Comparison of simulated flight data with time histories computed by using the estimation results. $\alpha = 10^0$; sea level.



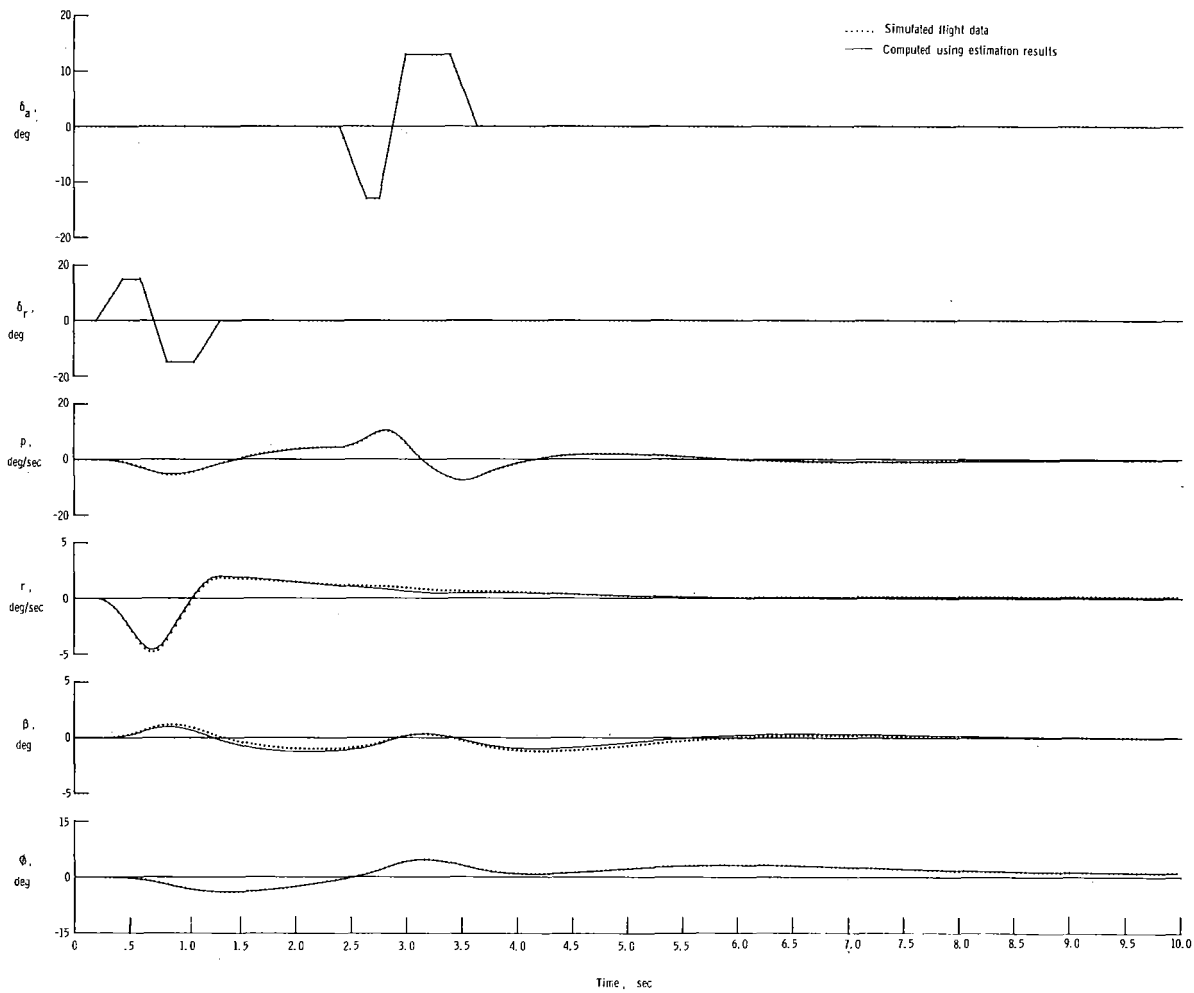
(b) Unmodeled $\dot{\beta}$ effects.

Figure 5.- Concluded.



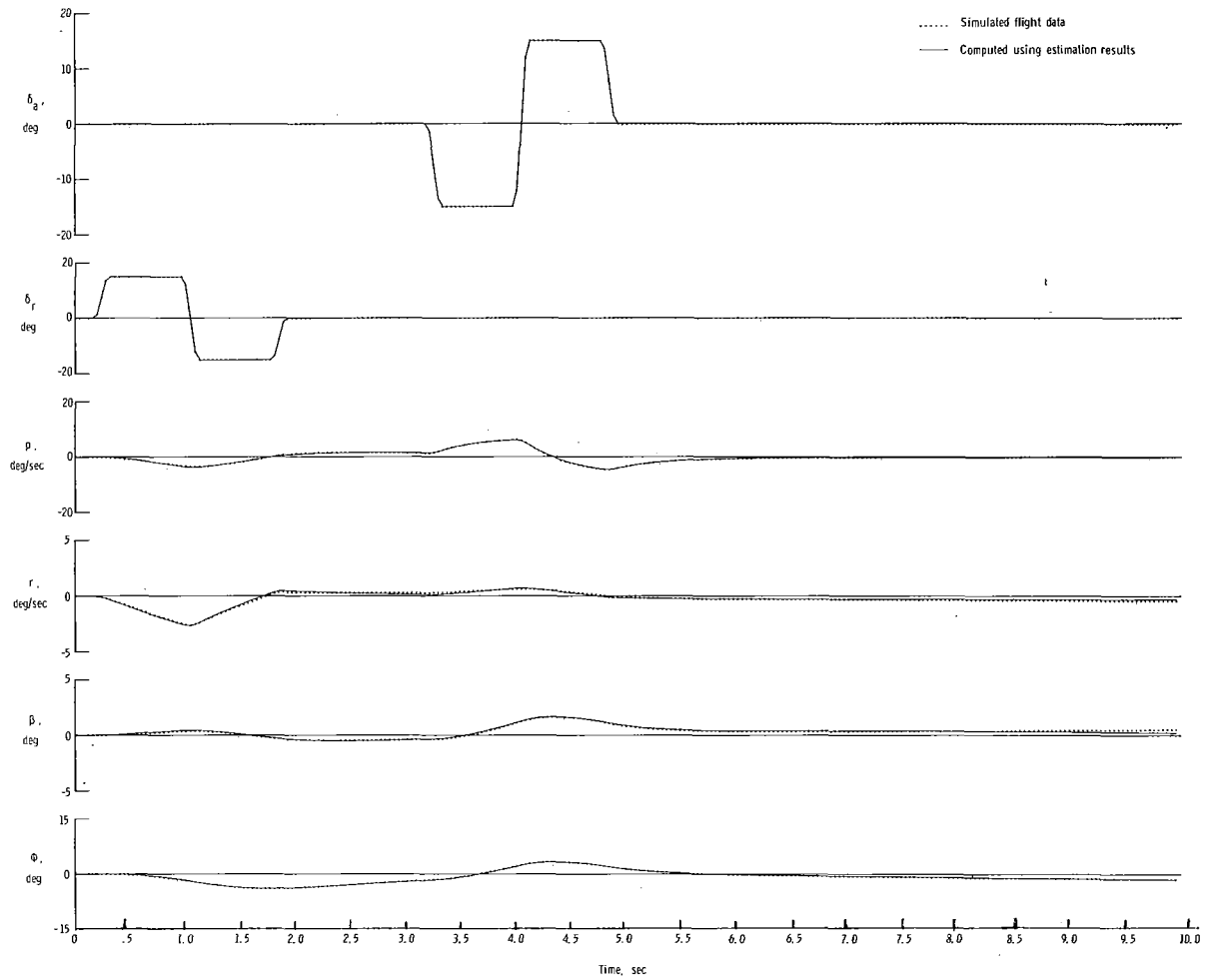
(a) Modeled $\dot{\beta}$ effects.

Figure 6.- Comparison of simulated flight data with time histories computed by using the estimation results. $\alpha = 20^\circ$; sea level.



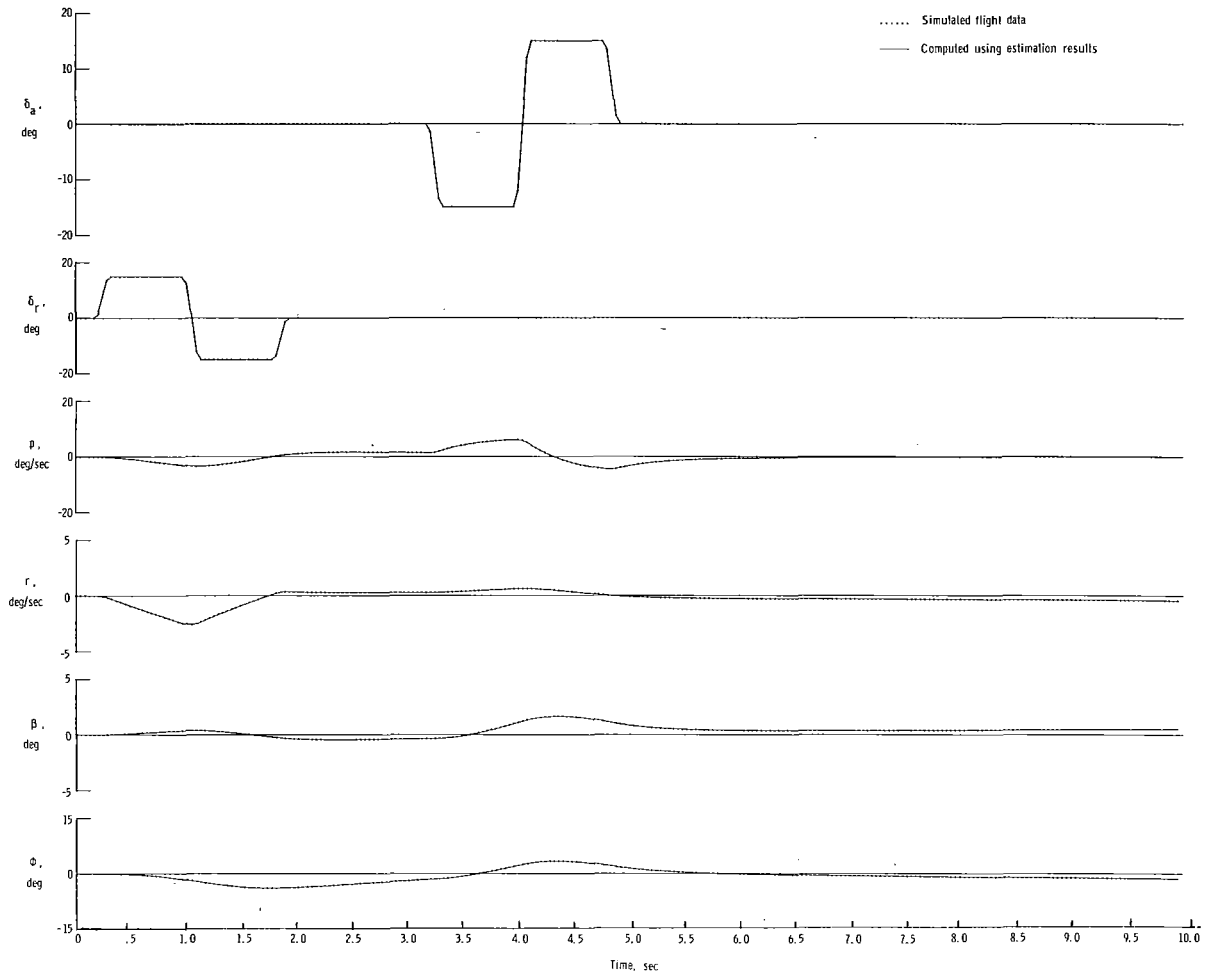
(b) Unmodeled $\dot{\beta}$ effects.

Figure 6.- Concluded.



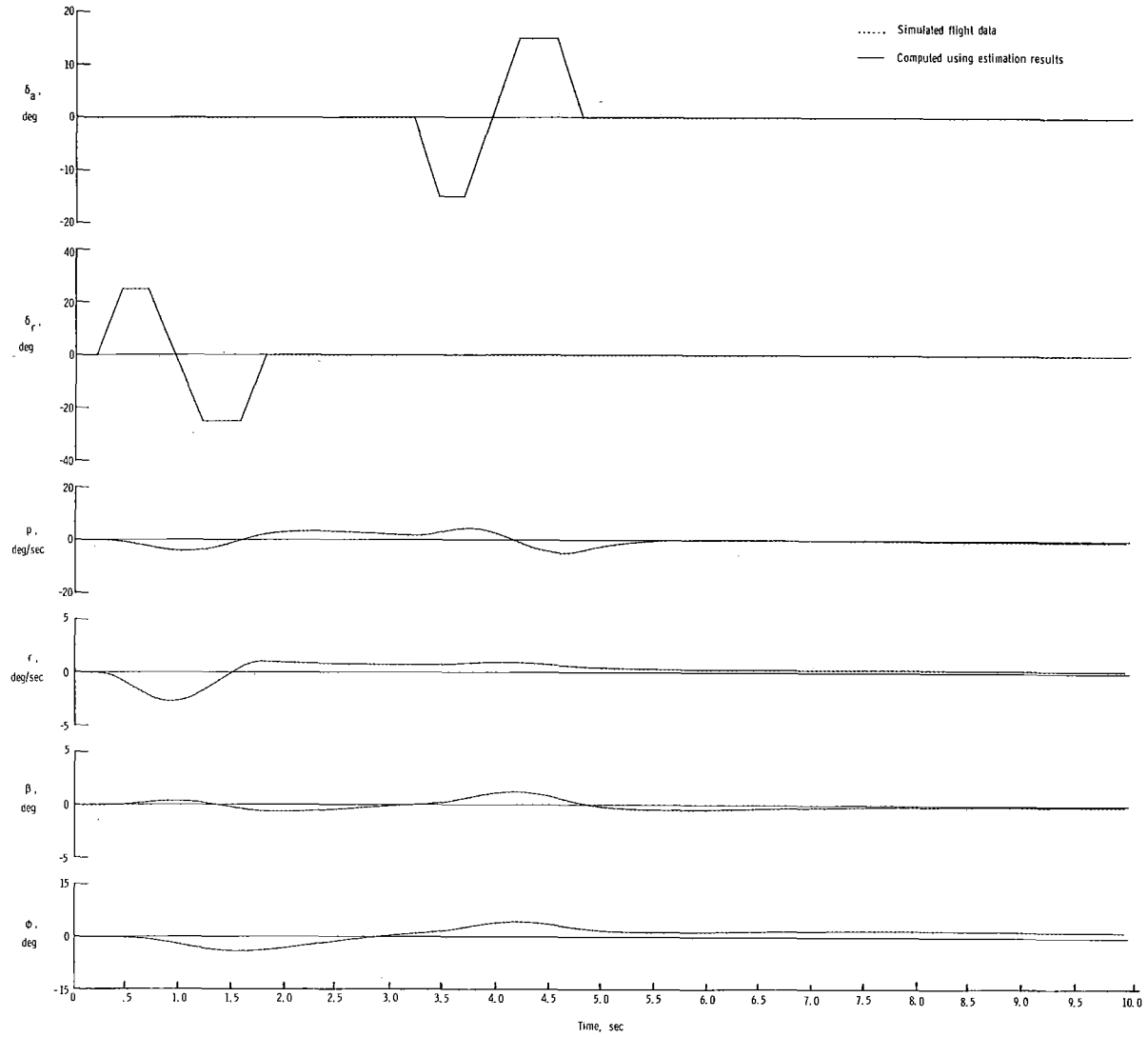
(a) Modeled $\dot{\beta}$ effects.

Figure 7.- Comparison of simulated flight data with time histories computed by using estimation results. $\alpha = 30^\circ$; case (a); sea level.



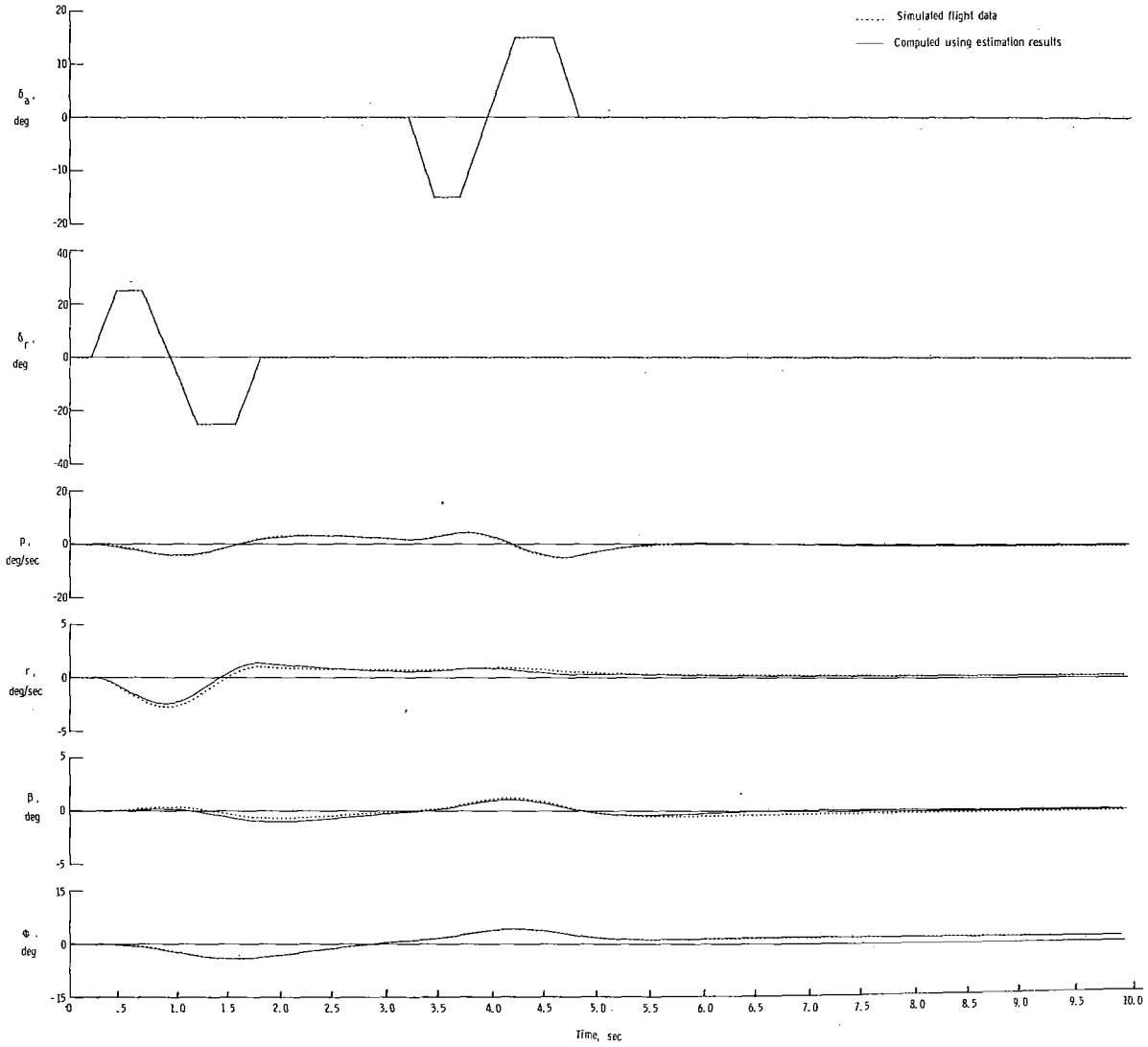
(b) Unmodeled $\dot{\beta}$ effects.

Figure 7.- Concluded.



(a) Modeled $\dot{\beta}$ effects.

Figure 8.- Comparison of simulated flight data with time histories computed by using estimation results. $\alpha = 30^\circ$; case (b); sea level.



(b) Unmodeled $\dot{\beta}$ effects.

Figure 8.- Concluded.

- Actual value
 - Estimated with modeled $\dot{\beta}$ effects
 - Estimated without $\dot{\beta}$ effects
 - ◇ Combined derivatives
- Unflagged symbols denote case (a) at $\alpha = 30^\circ$
 Flagged symbols denote case (b) at $\alpha = 30^\circ$

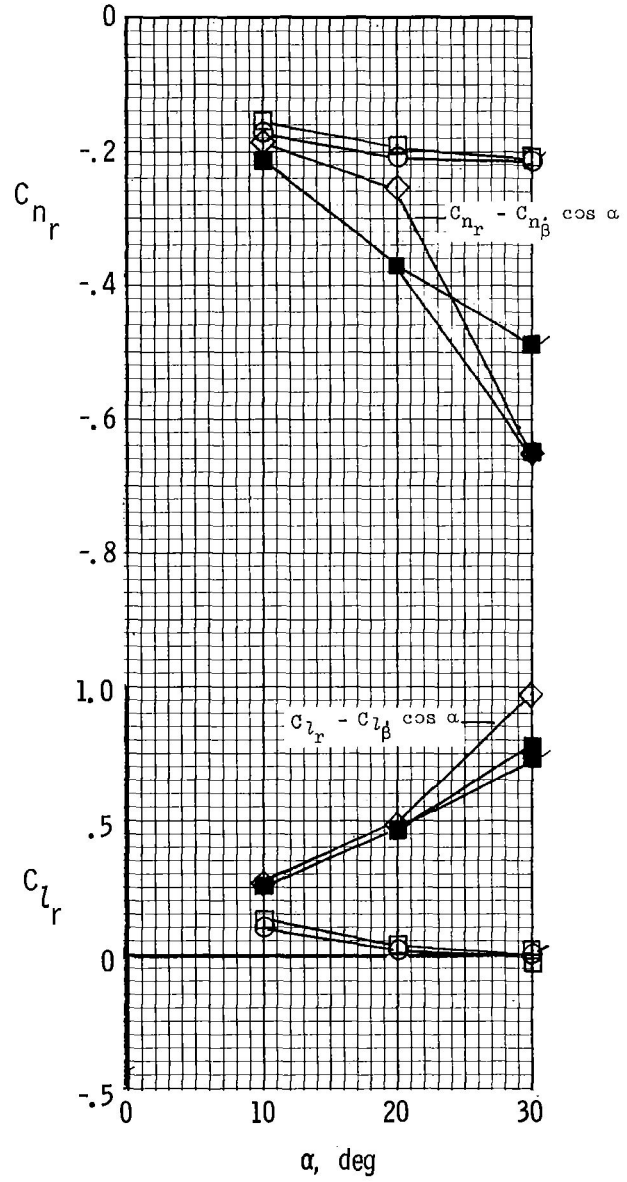
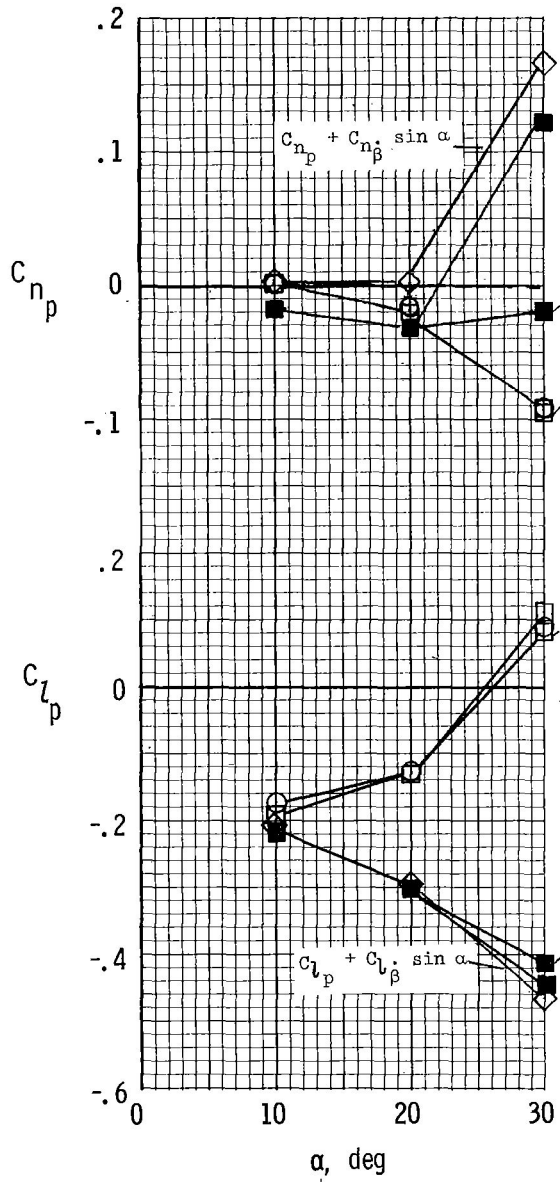


Figure 9.- Comparison of estimated aerodynamic derivatives with actual values. $h = 0$.

- Actual value
- Estimated with modeled β effects
- Estimated without β effects
- Unflagged symbols denote case (a) at $\alpha = 30^\circ$
- Flagged symbols denote case (b) at $\alpha = 30^\circ$

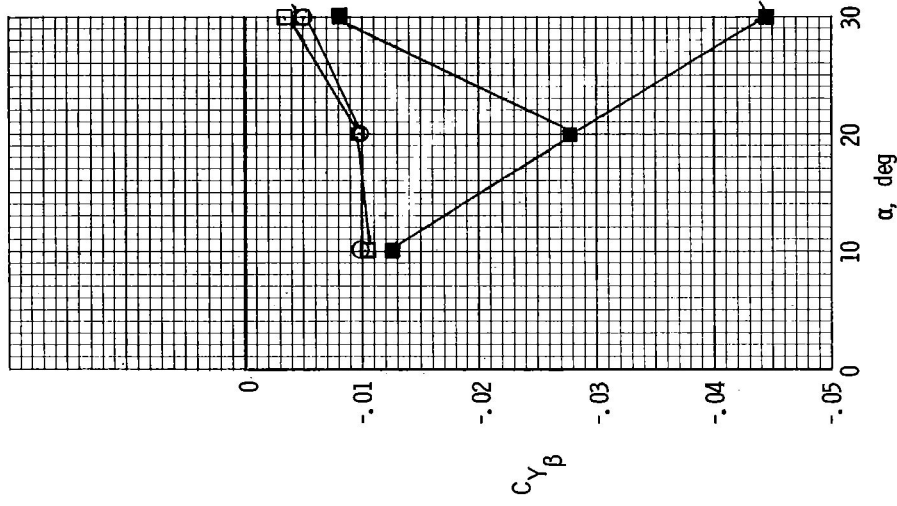
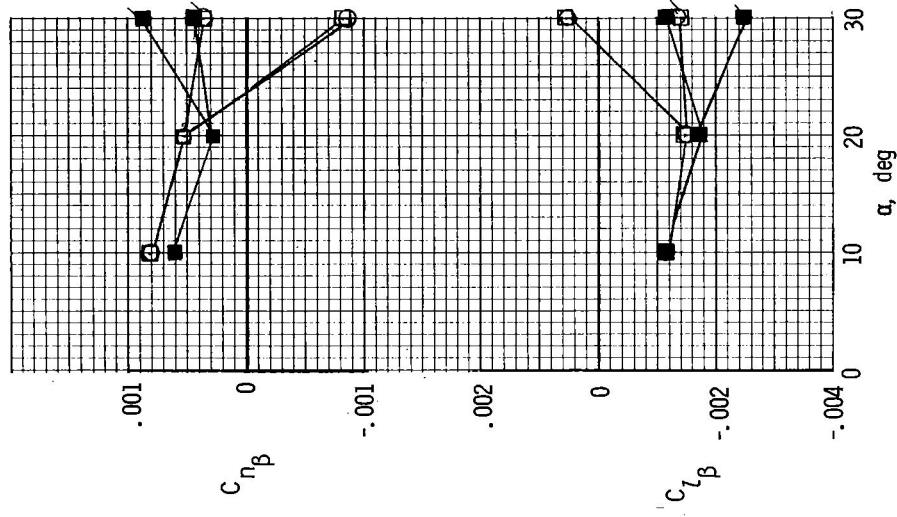
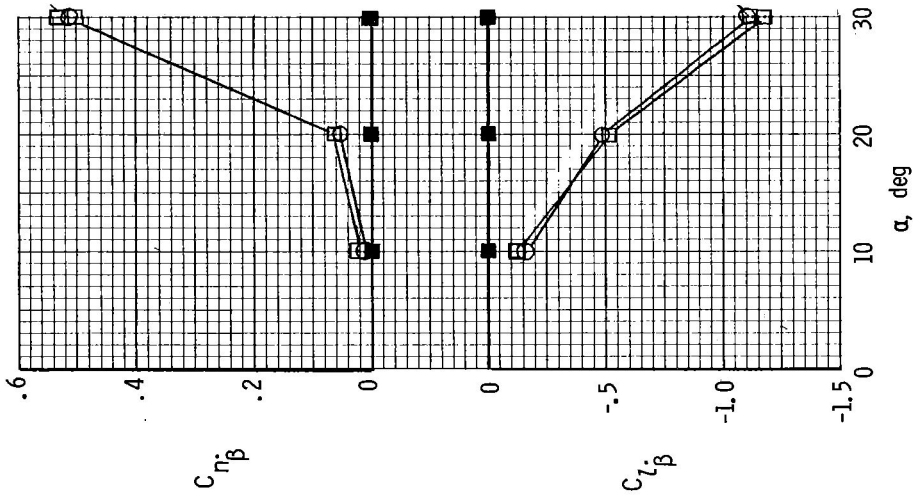


Figure 9.- Continued.

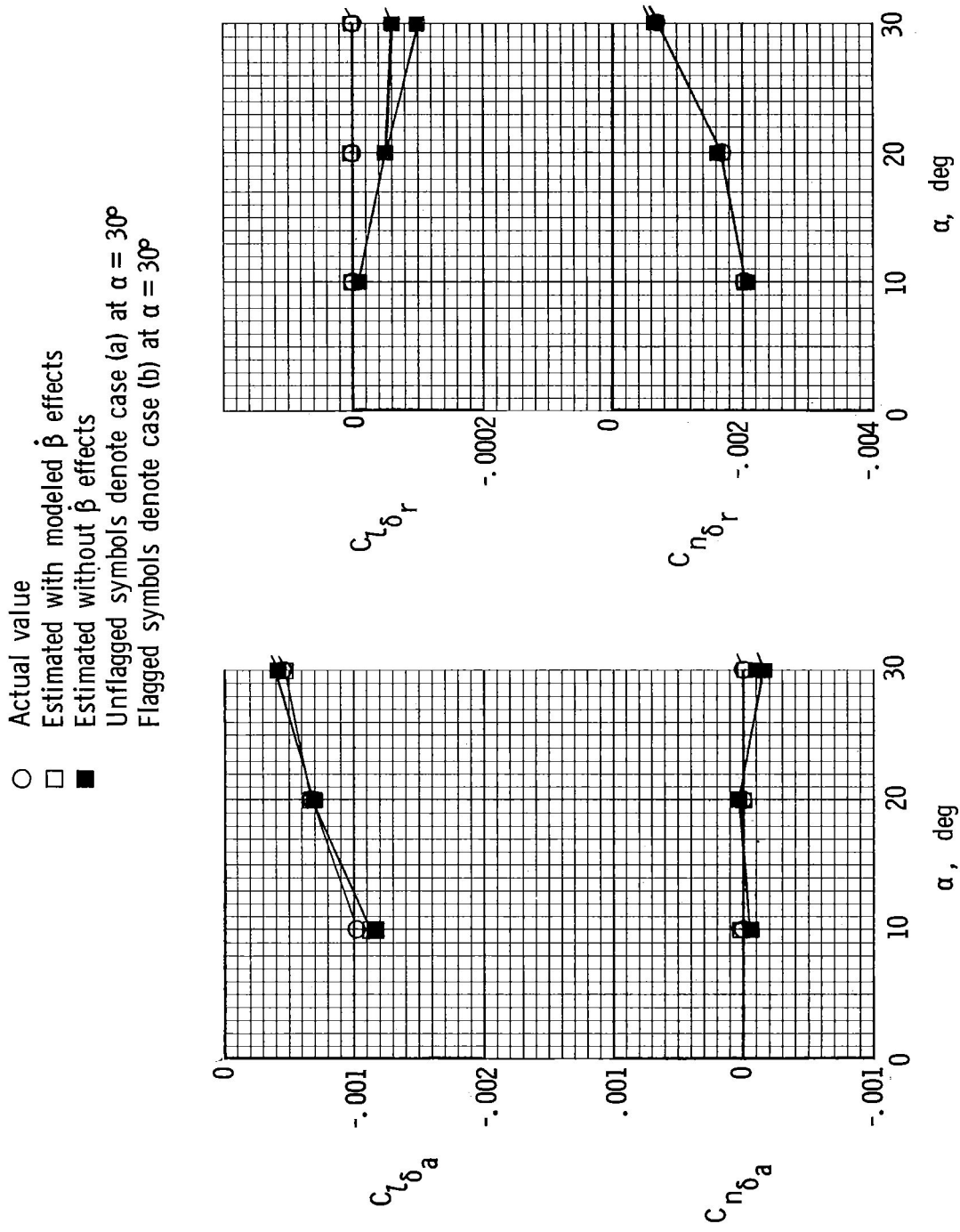


Figure 9.- Concluded.

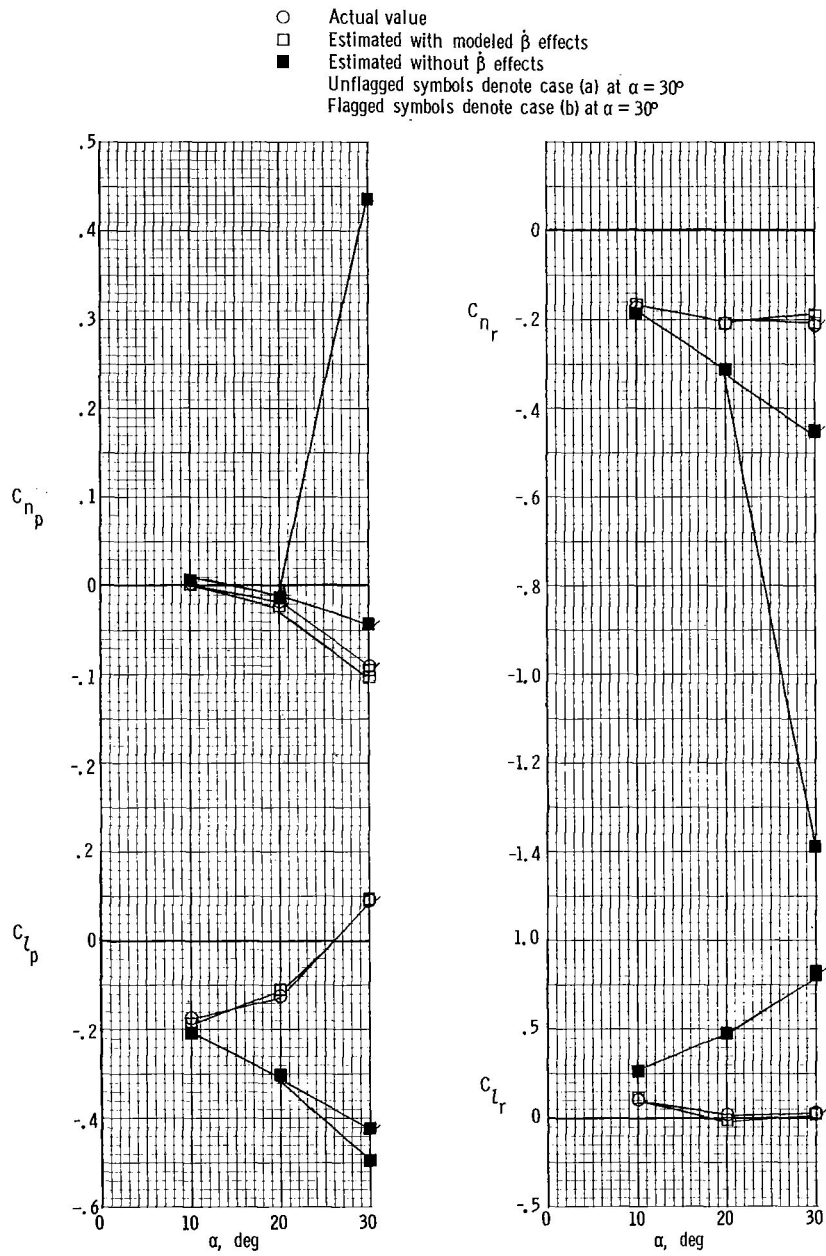


Figure 10.- Comparison of estimated aerodynamic derivatives with actual values. $h = 7620$ m (25 000 ft).

- Actual value
- Estimated with modeled $\hat{\beta}$ effects
- Estimated without $\hat{\beta}$ effects
- Unflagged symbols denote case (a) at $\alpha = 30^\circ$
- Flagged symbols denote case (b) at $\alpha = 30^\circ$

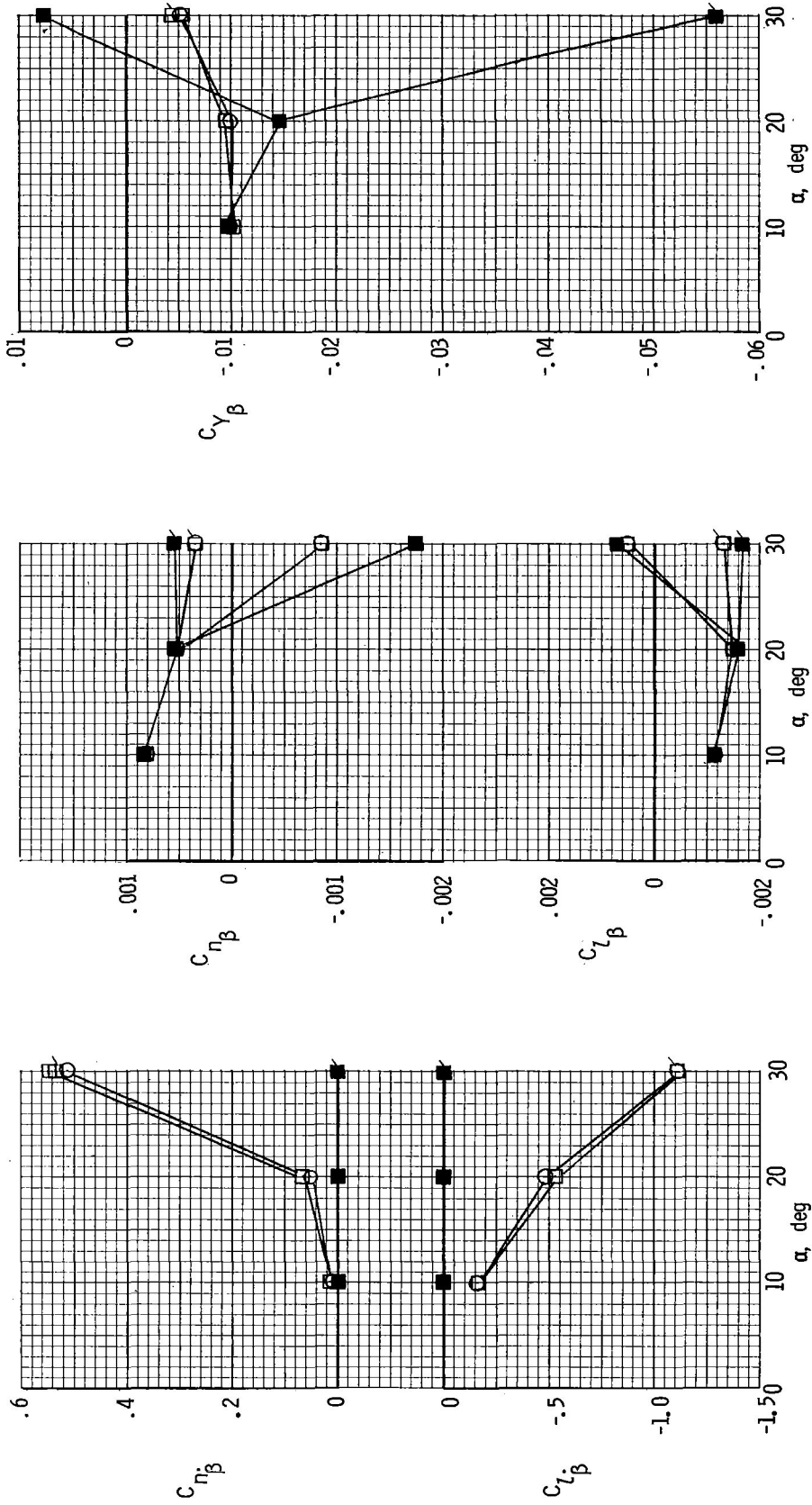


Figure 10.- Continued.

- Actual value
- Estimated with modeled β effects
- Estimated without β effects
- Unflagged symbols denote case (a) at $\alpha = 30^\circ$
- Flagged symbols denote case (b) at $\alpha = 30^\circ$

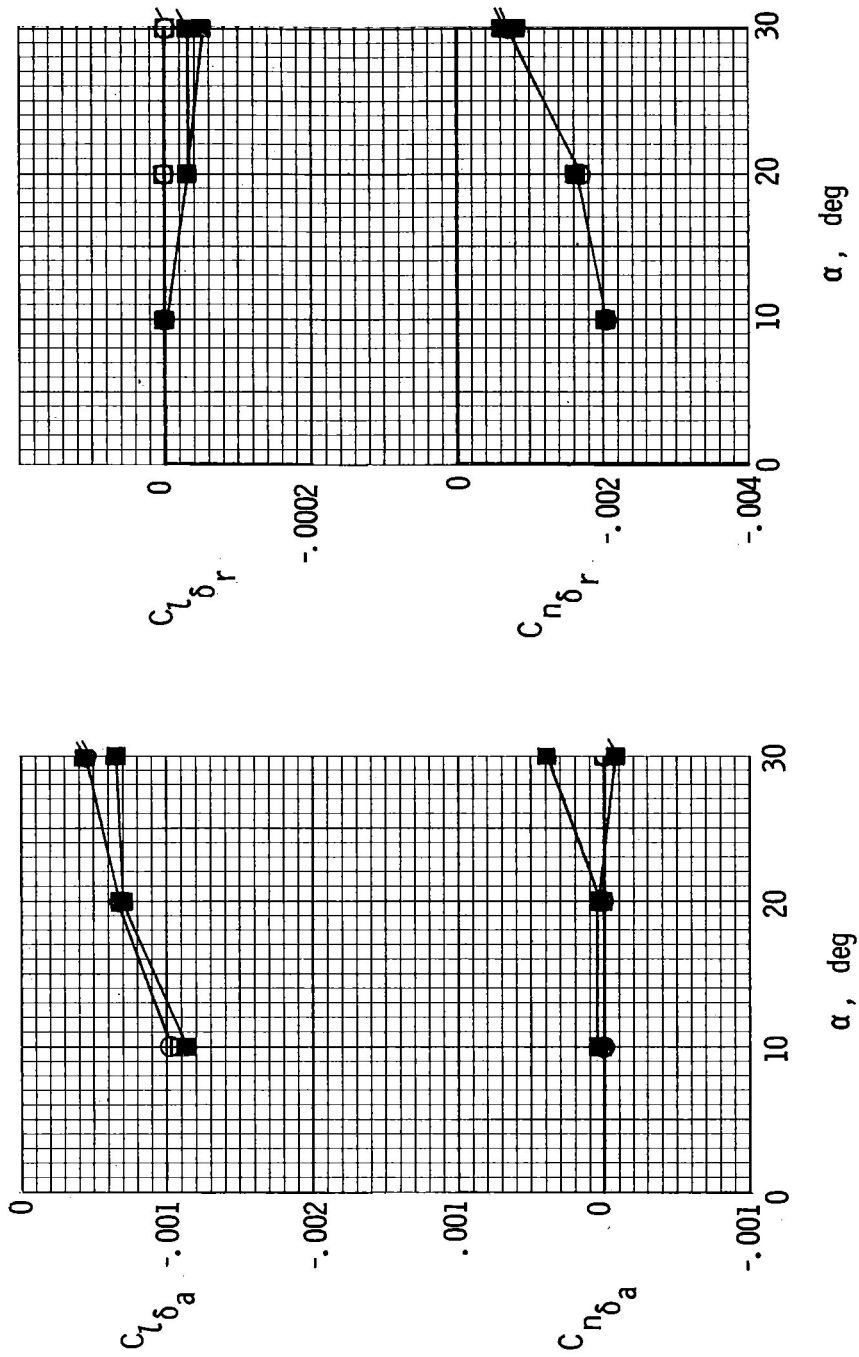


Figure 10.- Concluded.

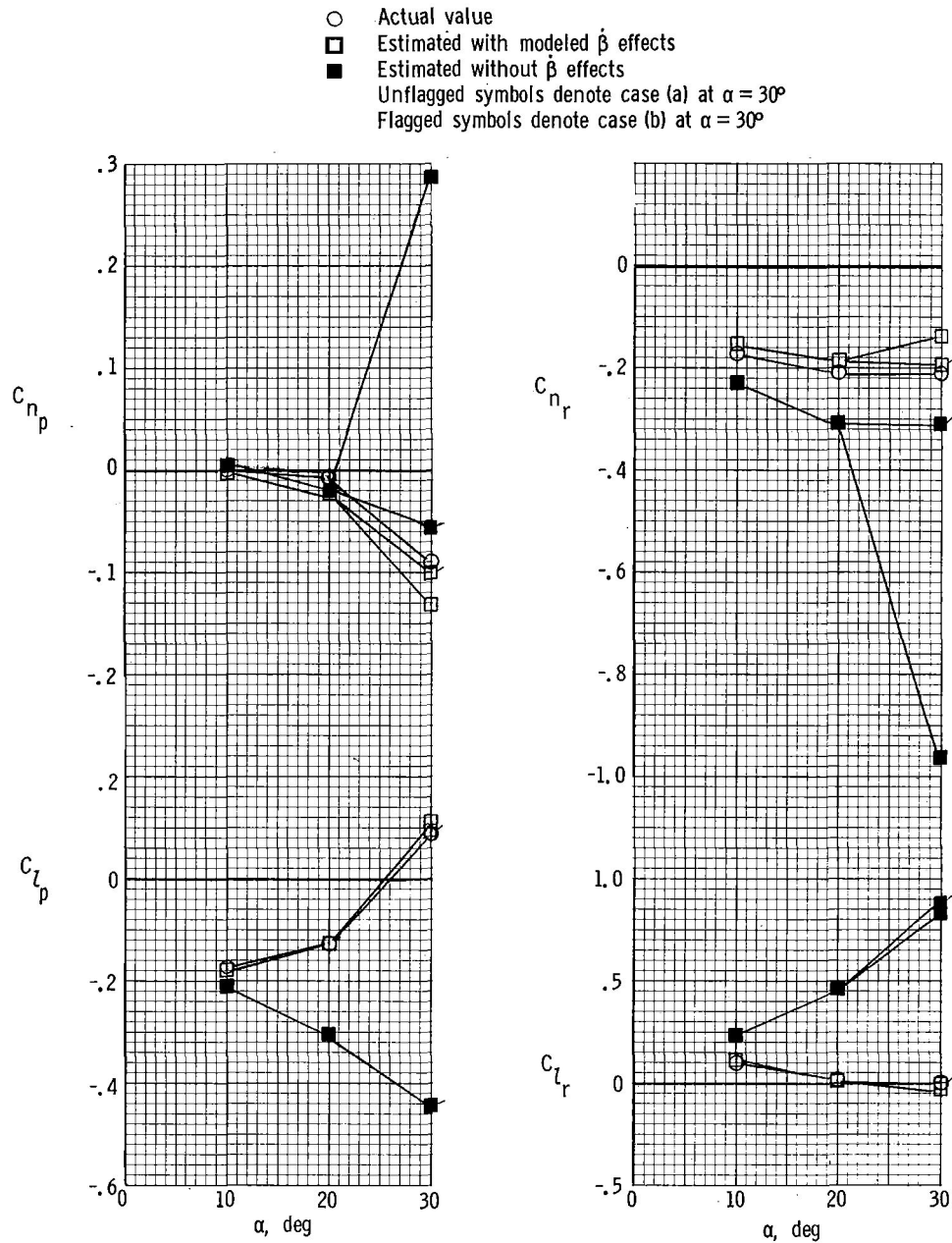


Figure 11.- Comparison of estimated aerodynamic derivatives with actual values. $h = 15\,240\text{ m}$ (50 000 ft).

- Actual value
- Estimated with modeled β effects
- ▣ Estimated without β effects
- Unflagged symbols denote case (a) at $\alpha = 30^\circ$
- Flagged symbols denote case (b) at $\alpha = 30^\circ$

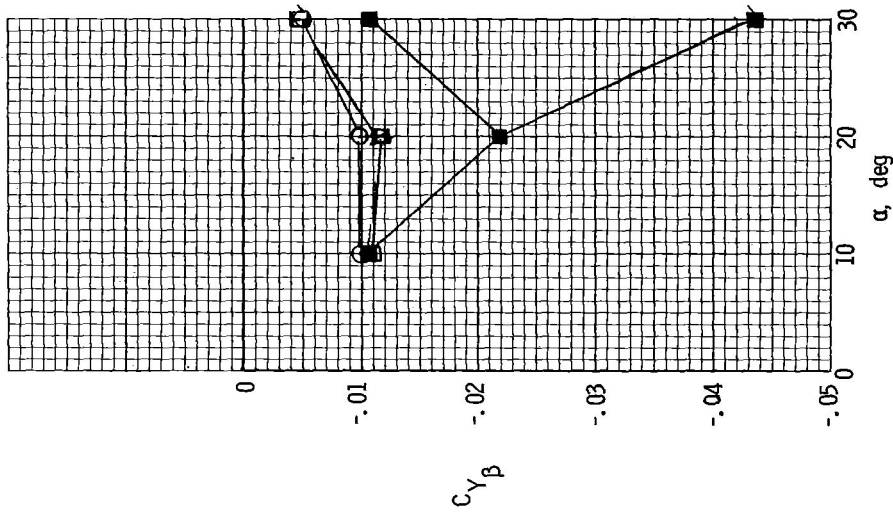
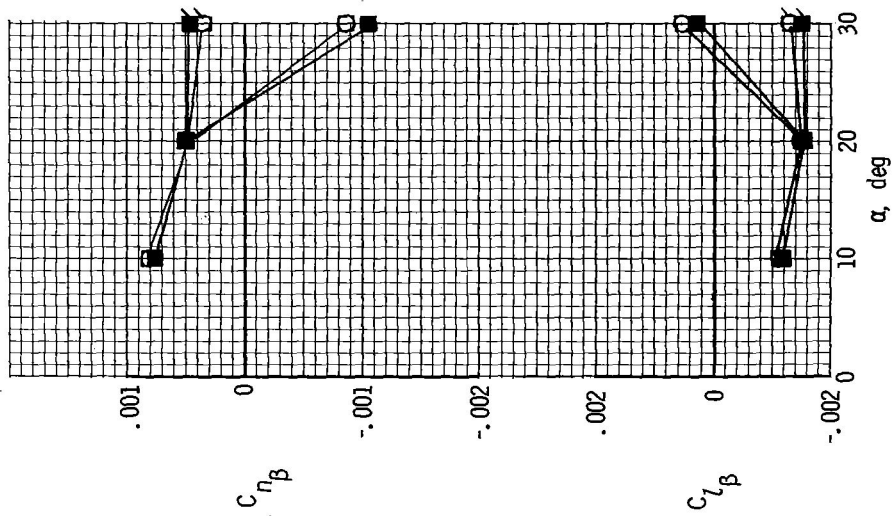
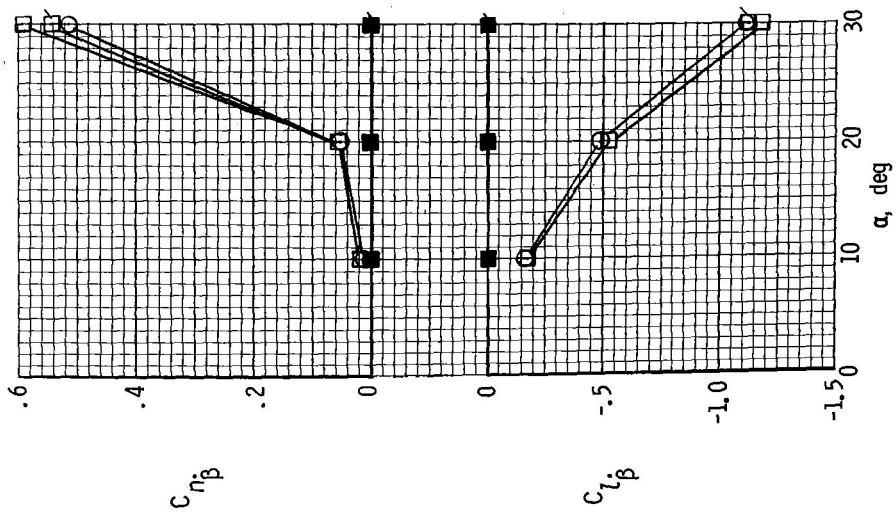


Figure 11.- Continued.

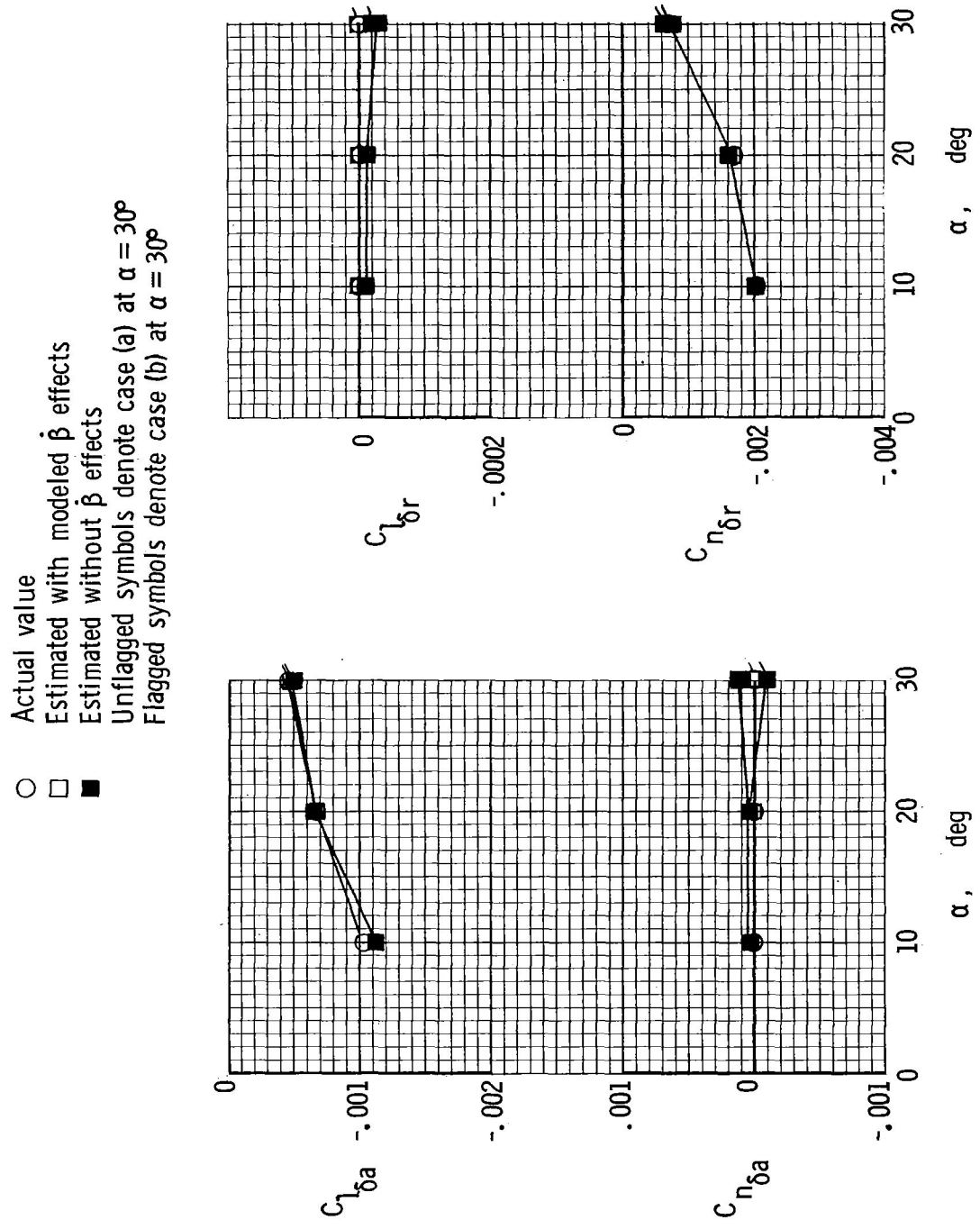


Figure 11.- Concluded.

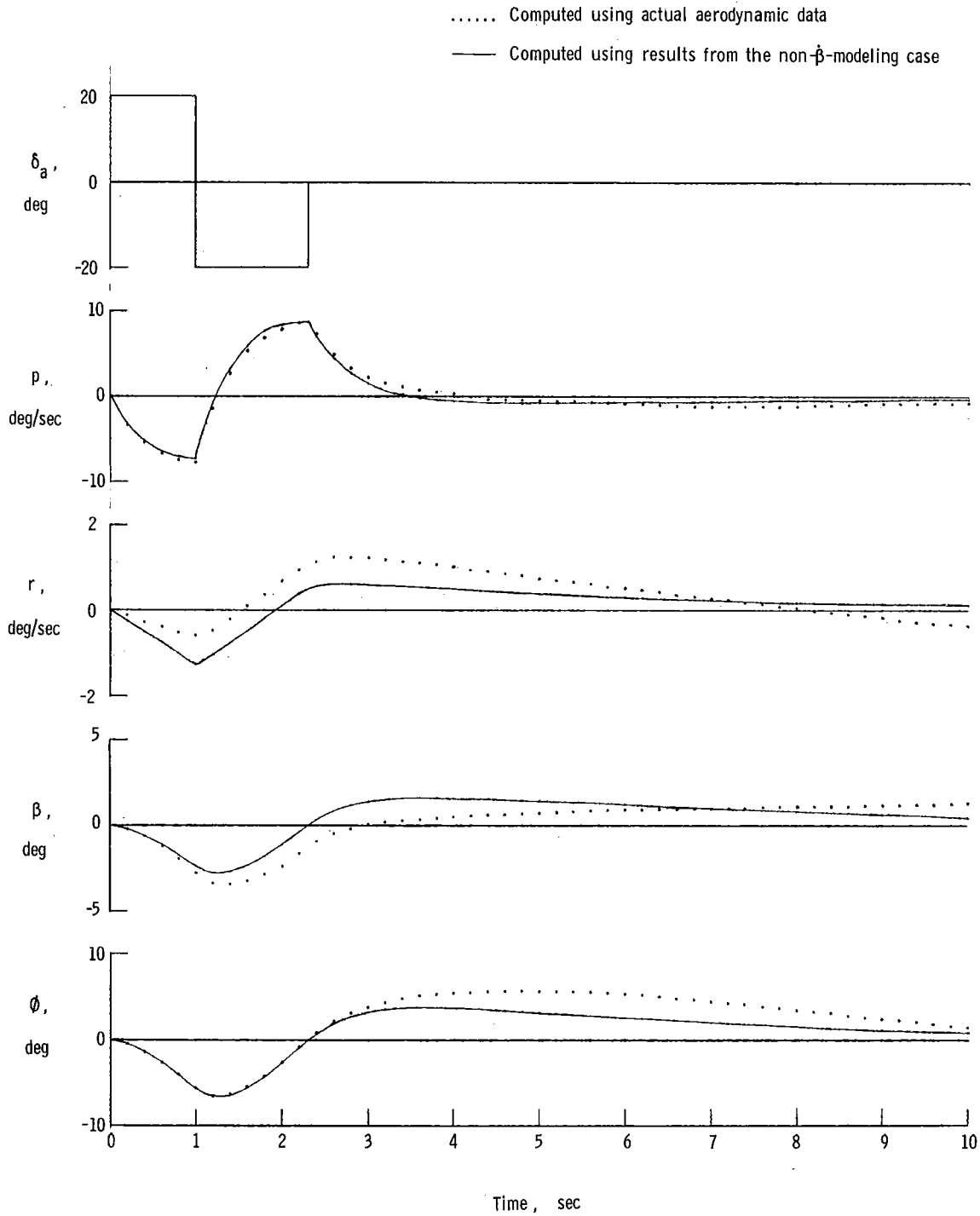


Figure 12.- Comparison of actual aileron doublet response with response computed by using the results from the unmodeled $\dot{\beta}$ effects estimation technique. $\alpha = 30^\circ$; case (a); sea level.



POSTMASTER : If Undeliverable (Section 158
Postal Manual) Do Not Return

"The aeronautical and space activities of the United States shall be conducted so as to contribute . . . to the expansion of human knowledge of phenomena in the atmosphere and space. The Administration shall provide for the widest practicable and appropriate dissemination of information concerning its activities and the results thereof."

—NATIONAL AERONAUTICS AND SPACE ACT OF 1958

NASA SCIENTIFIC AND TECHNICAL PUBLICATIONS

TECHNICAL REPORTS: Scientific and technical information considered important, complete, and a lasting contribution to existing knowledge.

TECHNICAL NOTES: Information less broad in scope but nevertheless of importance as a contribution to existing knowledge.

TECHNICAL MEMORANDUMS: Information receiving limited distribution because of preliminary data, security classification, or other reasons. Also includes conference proceedings with either limited or unlimited distribution.

CONTRACTOR REPORTS: Scientific and technical information generated under a NASA contract or grant and considered an important contribution to existing knowledge.

TECHNICAL TRANSLATIONS: Information published in a foreign language considered to merit NASA distribution in English.

SPECIAL PUBLICATIONS: Information derived from or of value to NASA activities. Publications include final reports of major projects, monographs, data compilations, handbooks, sourcebooks, and special bibliographies.

TECHNOLOGY UTILIZATION PUBLICATIONS: Information on technology used by NASA that may be of particular interest in commercial and other non-aerospace applications. Publications include Tech Briefs, Technology Utilization Reports and Technology Surveys.

Details on the availability of these publications may be obtained from:

SCIENTIFIC AND TECHNICAL INFORMATION OFFICE

NATIONAL AERONAUTICS AND SPACE ADMINISTRATION

Washington, D.C. 20546